

UNIVERSITÉ DU QUÉBEC À MONTRÉAL

ORIGINE DU CO₂ DANS LES FLUIDES PROFONDS DES CHAMPS
GÉOTHERMIQUES DU MEXIQUE

MÉMOIRE
PRÉSENTÉ
COMME EXIGENCE PARTIELLE
DE LA MAÎTRISE EN SCIENCES DE LA TERRE

PAR
LUC RICHARD

NOVEMBRE 2018

UNIVERSITÉ DU QUÉBEC À MONTRÉAL
Service des bibliothèques

Avertissement

La diffusion de ce mémoire se fait dans le respect des droits de son auteur, qui a signé le formulaire *Autorisation de reproduire et de diffuser un travail de recherche de cycles supérieurs* (SDU-522 – Rév.01-2006). Cette autorisation stipule que «conformément à l'article 11 du Règlement no 8 des études de cycles supérieurs, [l'auteur] concède à l'Université du Québec à Montréal une licence non exclusive d'utilisation et de publication de la totalité ou d'une partie importante de [son] travail de recherche pour des fins pédagogiques et non commerciales. Plus précisément, [l'auteur] autorise l'Université du Québec à Montréal à reproduire, diffuser, prêter, distribuer ou vendre des copies de [son] travail de recherche à des fins non commerciales sur quelque support que ce soit, y compris l'Internet. Cette licence et cette autorisation n'entraînent pas une renonciation de [la] part [de l'auteur] à [ses] droits moraux ni à [ses] droits de propriété intellectuelle. Sauf entente contraire, [l'auteur] conserve la liberté de diffuser et de commercialiser ou non ce travail dont [il] possède un exemplaire.»

REMERCIEMENTS

Je tiens à remercier mon directeur de recherche Daniele L. Pinti de la confiance qu'il m'a accordée en m'accueillant au sein de son équipe. Son soutien, ses conseils judicieux ainsi que ses multiples idées ont été indispensables à la réalisation de ma maîtrise.

Je souhaite également remercier mon codirecteur de recherche Jean-François Hélie pour sa disponibilité, ses conseils pratiques et sa pédagogie. Merci d'avoir pris le temps de m'expliquer la science derrière le fonctionnement des différents appareils de laboratoire et de m'avoir initié à leur entretien.

Merci à vous deux pour votre implication dans mon projet de recherche et pour les nombreuses connaissances que vous m'avez transmises. Ce fut une expérience très enrichissante et formatrice au monde de la recherche.

Je tiens à souligner l'intérêt envers mon projet d'études et la participation de Michel Préda par les analyses minéralogiques et cristallographiques réalisées. Un gros merci à mes collègues de bureau avec qui j'ai partagé tant de rires, de nourritures et de bons moments. Un merci plus particulier à Matthieu Moingt pour nos discussions scientifiques animées, ainsi que sa rigueur et ses conseils pratiques.

Merci à mes collègues de terrain Jonny Bahena Romero, Colin Ferguson et Sandra Nuñez avec qui j'ai partagé deux trop courtes semaines remplies de rires. Aye aye aye amigos !

Je remercie également la commission fédérale électrique (*Comision federal de electricidad* : CFE) du Mexique pour nous avoir permis d'échantillonner leurs champs géothermiques. Je tiens notamment à souligner l'hospitalité des membres de l'équipe de Cerro Prieto et Las Tres Vírgenes.

Les derniers remerciements appartiennent à ma famille pour leur soutien continu et leur encouragement dans les moments de doutes. Leur implication dans les différents projets de ma vie est sans faille, sans eux il m'aurait été difficile de finaliser celui-ci.

Merci à ma partenaire de vie, mon amie et ma confidente avec qui je partage tant d'amour et de bons moments. Tu m'as motivé à fournir les derniers efforts et tu me fais grandir.

AVANT-PROPOS

Ce mémoire s'inscrit dans le cadre du Projet 20 (évaluation du potentiel et de la surexploitation des puits géothermiques à l'aide des gaz rares) dirigé par la professeure Aida López Hernández de *l'Universidad Michoacana de San Nicolás de Hidalgo* pour le centre mexicain d'innovation en énergie géothermique (CeMIEGeo). Le financement a été entièrement assuré par le CONACYT (*Consejo Nacional de Ciencia y Tecnología de Mexico*). Ce mémoire a été rédigé sous forme d'article scientifique qui sera soumis au *Journal of Volcanology and Geothermal Research*. Cela dit la langue, la mise en forme et la méthode de citation sont celles demandées par le journal. J'ai effectué l'échantillonnage des champs géothermiques Cerro Prieto et Las Tres Virgenes avec l'aide de mes collègues cités dans les remerciements, des membres du personnel de la CFE (Comisión Federal de Electricidad) et de mon directeur de recherche Daniele L. Pinti lors de la campagne d'échantillonnage de novembre 2016 au Mexique. La campagne d'échantillonnage des champs géothermiques Los Azfures et Los Humeros avait préalablement été effectuée par le professeur Pinti, les membres de son groupe de recherche du moment ainsi que ceux de la CFE. Mon implication dans le projet a été d'effectuer le travail en laboratoire, l'interprétation des résultats et la rédaction de l'article scientifique pour la partie isotope stable du CO₂. Mes directeurs de recherche ont supervisé l'ensemble du travail et révisé l'article scientifique.

TABLE DES MATIÈRES

REMERCIEMENTS.....	iii
AVANT-PROPOS	v
LISTE DES FIGURES	ix
LISTE DES TABLEAUX	xi
LISTE DES ABRÉVIATIONS, SIGLES ET ACRONYMES.....	xiii
LISTE DES SYMBOLES.....	xvii
RÉSUMÉ	xix
CHAPITRE I INTRODUCTION	1
CHAPITRE II DEEP CARBON IN GEOTHERMAL FIELDS OF MEXICO	3
2.0 Abstract.....	4
2.1 Introduction.....	7
2.2 Geology.....	9
2.2.1 The Cerro Prieto Geothermal Field (CP-GF)	10
2.2.2 Los Azufres Geothermal Field (LA-GF).....	12
2.2.3 Los Humeros Geothermal Field (LH-GF).....	13
2.2.4 Las Tres Vírgenes Geothermal Field (LTV-GF).....	15
2.3 Sampling and analytical methods	17
2.3.1 Sampling	17
2.3.2 Analytical methods	19
2.3.3 Assessment of the total method variability	19
2.4 RESULTS	22
2.5 DISCUSSION	24
2.5.1 Inter-field C and O isotopic variability	24
2.5.2 The O isotopic variability.....	25
2.5.3 The C isotopic variability	28

2.6 Conclusions	36
2.7 Acknowledgments.....	38
2.8 Appendix	39
2.9 References	41
2.10 Figures and table	56
CHAPITRE III CONCLUSION GÉNÉRALE	67
LISTE DES RÉFÉRENCES	71

LISTE DES FIGURES

Figure		Page
2.0.	Graphical Abstract. Distinct isotopic composition of carbon and oxygen in CO ₂ from production wells, hot springs and fumaroles of Mexican geothermal fields. The values in each field is discretely highlighted by ellipsoids of different colors which represents the total method variability around a mean value which is represented by the cross sign.	6
2.A.1	Sample internal pressure versus the CO ₂ isotopic composition. The solid line is the linear correlation between the sample internal pressure and the δ ¹⁸ O-CO ₂ while the dash line represents the 2bar threshold.	39
2.1	Location of the geothermal fields sampled for this study with main geodynamic features of the region. TMVB is the Trans-Mexican Volcanic Belt interpreted as the surface expression of the present-day subduction of the Cocos Plate. The Comondù arc centers are intrusions related to Miocene-time subduction which is now inactive and replaced by the Gulf of California opening. The A-A' is the transect of the lithospheric cross section of Figure 2.8.	56
2.2	Geothermal well platform sketch showing the Webre separator, the silencer and the weirbox, with the position where gas (point A) and water (point B) samples were taken.	57
2.3	The C and O isotopic composition measured in the four geothermal fields. Ellipsoids of different colors represents the total method variability around a mean value which is represented by the cross sign.	58
2.4	Comparison between the carbon isotopic composition, expressed as δ ¹³ C (‰ vs VPDB) measured in the four geothermal fields in this study and previous literature data. To notice the extreme lighter values measured in Los Azufres by Birkle et al. (2001) which might indicate organic contamination during sampling or during analyses.	59
2.5	The O isotopic composition of geothermal water and CO ₂ (both normalized to VSMOW) in the different geothermal field. The general trend indicates that equilibration between the two phases basically controls the oxygen	

	isotopic signature. Scattering indicates likely the overlapping with other local processes such as exchange with silicates and carbonates in the reservoir. ..	60
2.6	The per mil fractionation of the CO ₂ -H ₂ O phase equilibration calculated at different temperatures. The curve of Chiodini et al. (2000) is calculated based on data from hot springs. The Richet et al. (1977) curve is theoretical. The boxes represent the possible range per mil fractionation between CO ₂ and H ₂ O in the four geothermal fields studied, calculated at well separation temperatures. The data of Panichi et al. (1977) for Larderello field, Italy, is also reported for comparison.	61
2.7	Atmosphere-corrected ³ He/ ⁴ He ratio measured in geothermal fluids of Mexico expressed as ratio Rc normalized to the atmospheric one Ra (= 1.384 x 10 ⁻⁶ ; Lupton et al., 1976) versus the δ ¹³ C-CO ₂ measured in the same wells (see text for data sources). The dashed lines represent hyperbolas of mixing between the MORB mantle source and organic matter (OM) rich sediments and carbonates. Hyperbola curvature “r” is equal to the ratio (C/He) _{mantle} /(C/He) _{organic/carbonate} . Note that the Y-axis is split for sake of clarity.	62
2.8	Cross section of the Coco plate subduction zone at the level of Mexico City (adapted from Pérez-Campo et al., 2008) with the relative position of the Trans Mexican Volcanic Belt (TMVB) and the geothermal fields of Los Azufres (LA) and Los Humeros (LH). Blobs of mantle material of different nature (fertilized mantle = orange and lithospheric mantle = red) are reported as possible sources of He and C in the two fields.....	63

LISTE DES TABLEAUX

Tableau	Page
2.A.1 Repeated analyses of CO ₂ isotopes in Cerro Prieto wells to test analytical consistency	40
2.A.2 Measurements of oxygen isotopic signature in condensate water and steam from the same sampling tube.....	40
2.1 The geothermal field sampled, the type of fluid collected, the year of sampling and the, δ ¹³ C-CO ₂ , δ ¹⁸ O-CO ₂ (with their analytical uncertainties).	64

LISTE DES ABRÉVIATIONS, SIGLES ET ACRONYMES

CONACYT	<i>Consejo Nacional de Ciencia y Tecnología</i> Conseil nationale de science et technologie
CP	<i>Cerro Prieto</i>
CFE	<i>Comisión Federal de Electricidad</i> Commission fédérale électrique
E.g.	<i>Exempli gratia</i> Par exemple
Et al.	<i>Et alli</i> Et autres
GF	<i>Geothermal field</i> Champ géothermique
GMWL	<i>Global Meteoritic Water Line</i> Droite des eaux météoritiques

I.e.	<i>Id est</i>
	C'est-à-dire
IRMS	<i>Isotop ratio mass spectrometer</i>
	Spectromètre de masse à ratio isotopique
LA	<i>Los Azufres</i>
LH	<i>Los Humeros</i>
LSVEC	<i>Lithium carbonate prepared by H. Svec</i>
	Carbonate de lithium préparé par H. Svec
LTV	<i>Las Tres Virgenes</i>
MORB	<i>Mid Ocean Ridge Balsalt</i>
	Basalte de ride médio-océanique
NPZ	<i>Nothern Production Zone</i>
	Zone de production du Nord
OM	<i>Organic Matter</i>
	Matière organique

PETM	<i>Paleocene-Eocene thermal maximum</i>
	Maximum thermique de la transition Paléocène-Éocène
SPZ	<i>Southern Production Zone</i>
	Zone de production du Sud
Sr	Strontium
TMVB	<i>Trans Mexican Volcanic Belt</i>
	Ceinture de roches volcaniques transMexicaine
VSMOW	<i>Vienna Standard mean ocean water</i>
	Eau océanique moyenne normalisée de Vienne
VPDB	<i>Vienna Pee Dee Belemnite</i>
	Bélemnite de Pee Dee normalisé à Vienne

LISTE DES SYMBOLES

C Carbone

CH₄ Méthane

CO₂ Dioxyde de carbone

cm Centimètre

°C Degré Celsius

δ Delta

~ Environ

H₂O Eau

He Hélium

Km Kilomètre

O	Oxygène
>	Plus grand que
±	Plus ou moins
<	Plus petit que
"	Pouce
%	Pour mille

RÉSUMÉ

Les champs géothermiques (GFs) offrent une fenêtre géologique de plus de 4 km de profondeur sur le « carbone profond ». Le cycle « géologique » du carbone est encore mal caractérisé, bien qu'il ait engendré certains des changements climatiques les plus drastiques à l'échelle des temps géologiques, tels que la sortie de « snowball earth » et le maximum thermique du Paléocène-Éocène (PETM). Face aux changements climatiques actuels, il est devenu nécessaire de caractériser l'ensemble des sources d'émission de carbone anthropique et naturel. Ce projet de maîtrise s'inscrit dans un effort d'amélioration des connaissances sur le carbone profond en fournissant une étude complète de l'origine et du comportement du carbone en contexte géothermal.

Une vaste campagne d'échantillonnage a été déployée entre 2014 et 2016 dans les GFs de « haute température » ($> 200^{\circ}\text{C}$) de Cerro Prieto (CP-GF), Los Azufres (LA-GF), Los Humeros (LH-GF) et Las Tres Virgenes (LTV-GF). La composition isotopique de l'oxygène et du carbone du CO₂ a permis de distinguer pour une première fois les fluides de chaque GF. Les résultats ont démontré que la source du C de l'ensemble des GFs est principalement mantellique. Elle est donc comparable à celle qui alimente les basaltes de ridges médio-océaniques (MORBs). Cependant, et grâce à des comparaisons entre la composition isotopique du carbone ($d^{13}\text{C}$) et celle de l'hélium (${}^3\text{He}/{}^4\text{He}$) on observe une contribution en C qui provient d'un échange isotopique avec des carbonates à LH-GF et de la matière organique à LTV-GF.

La composition isotopique de l'oxygène du CO₂ est dépendante de la source initiale d'eau alimentant les fluides géothermiques et des processus d'équilibrations subséquents. Une équilibration partielle entre l'oxygène de la molécule d'eau et du CO₂ au séparateur a été observée alors que des recherches précédentes indiquent un équilibre complet. Il est intéressant de noter que la réinjection des fluides dans un réservoir géothermique déplace la composition isotopique de l'eau vers des valeurs plus élevées. C'est notamment le cas au CP-GF qui semble maintenant être un mélange d'eau météoritique et andésitique plutôt que magmatique. L'évolution des fluides au CP-GF induit également un rapport ${}^3\text{He}/{}^4\text{He}$ plus faible que prévu dans un contexte de « pull-apart ». Il a été proposé par Pinti (2018) que cette anomalie soit causée par la production de ${}^4\text{He}$ par désintégration d'uranium et de thorium dans le réservoir confiné du CP-GF.

Mots-clés : carbone profond; dioxyde de carbone, isotopes du carbone, isotopes de l'oxygène; isotopes de l'hélium; systèmes géothermaux

CHAPITRE I

INTRODUCTION

Le réchauffement climatique est l'un des enjeux les plus importants auxquels l'homme fait actuellement face. Le flux de carbone anthropique représente aujourd'hui plus de 10 fois celui du carbone naturellement émis durant le maximum thermique de la transition Paléocène-Éocène (PETM) (Zeebe, Ridgwell et Zachos, 2016). Ces émissions naturelles ont suffi à engendrer un réchauffement climatique de ~5-8 °C ainsi qu'un grand bouleversement de la biodiversité (McInerney et Wing, 2011). Il est donc primordial de caractériser les sources anthropiques et naturelles du dioxyde de carbone (CO₂).

Arrhenius (1896) et Chamberlain (1899) furent parmi les premiers à proposer l'incidence du CO₂ sur le climat. Par la suite, les travaux de Keeling (1960) consistant à mesurer de façon continue les concentrations de CO₂ atmosphérique ont avivé l'intérêt scientifique. Cela a donc permis de dresser un portrait pragmatique du bilan carbone de l'exosphère (e. g. Post *et al.*, 1990; Cox *et al.*, 2000; Boesch *et al.*, 2011; Le Quéré *et al.*, 2018). On sait aujourd'hui que le carbone mantellique a amorcé des changements climatiques drastiques au cours des temps géologiques tels que la sortie de « Snowball earth » (Hoffman *et al.*, 1998) et le PETM (Zachos *et al.*, 2005). Cependant, le cycle géologique du dit « carbone profond » est encore mal défini, car ce n'est que très récemment que les scientifiques ont cherché à approfondir leurs connaissances sur ce cycle (Dasgupta et Hirschmann, 2010).

Ainsi, cette maîtrise a comme objectif principal de contribuer à accroître les connaissances sur le carbone profond en fournissant une étude complète de l'origine et du comportement du carbone en contexte géothermal. En plus d'être une source énergétique alternative et moins polluante, les champs géothermiques offrent une fenêtre géologique d'une profondeur de plus de 4 km sur le carbone. Le CO₂ contenu dans les fluides extraits de champs géothermiques représente souvent plus de 90 % de la phase volatile sèche (Birkle *et al.*, 2001 ; Verma *et al.*, 2006). Nous avons donc mesuré les compositions isotopiques du CO₂ ($\delta^{18}\text{O-CO}_2$; $\delta^{13}\text{C-CO}_2$) et de l'H₂O ($\delta^2\text{H-H}_2\text{O}$; $\delta^{18}\text{O-H}_2\text{O}$) des fluides de quatre champs géothermiques mexicains présentement en exploitation pour la production d'électricité par la *Comisión Federal de Electricidad* (CFE), soit Cerro Prieto, Los Azufres, Los Humeros et Las Tres Virgenes (CP, LA, LH et LTV-GF). Les sources et comportement du carbone dans ces réservoirs ont donc été documentés et les résultats principaux de cette maîtrise sont ci-exposés sous forme d'un article scientifique qui sera soumis au *Journal of Volcanology and Geothermal Research*.

CHAPITRE II

DEEP CARBON IN GEOTHERMAL FIELDS OF MEXICO

LUC RICHARD^{*1}, DANIELE L. PINTI¹, JEAN-FRANÇOIS HÉLIE¹, AIDA
LÓPEZ HERNÁNDEZ², MARIA CLARA CASTRO³

¹GEOTOP RESEARCH CENTER ON THE DYNAMICS OF THE EARTH
SYSTEM, UNIVERSITÉ DU QUÉBEC À MONTRÉAL, H3X 3Y7, QC, CANADA

²Facultad de Ingeniería Civil, Universidad Michoacána de San Nicolas de Hidalgo
(UMSNH), Morelia, Mich., México

³Department of Earth and Environmental Sciences, University of Michigan, Ann
Arbor, MI, USA

* Corresponding author: Richard.luc.9@gmail.com +1 514 265 2795

Prepared for submission to Journal of Volcanology and Geothermal Research

Keywords: Deep carbon; carbon dioxide; carbon isotopes; oxygen isotopes; helium
isotopes; geothermal systems.

2.0 Abstract

An extensive sampling campaign has been carried out between 2014 and 2016 at the Cerro Prieto (CP), Los Azufres (LA), Los Humeros (LH) and Las Tres Vírgenes (LTV) geothermal fields, Mexico. The geothermal fields of LA and LH are situated in an arc magmatism context related to the Cocos plate subduction under the North American one. CP and LTV are presently located in extensional contexts of pull-apart related to the San Andreas fault system and of the opening of Gulf of California, respectively. The aim of the study was to determine the origin of C in CO₂ and its behavior in ‘high temperature’ (> 200°C) geothermal sedimentary and volcanoclastic reservoirs. The most interesting feature observed in this study is that the measured isotopic composition of CO₂ (¹³C/¹²C and ¹⁸O/¹⁶O ratios) is distinct and unique for each sampled geothermal field. The isotopic variability of carbon is controlled by its sources (i.e., δ¹³C value: -6±2‰ in mantle; -20‰ in carbon organic matter-rich sediments; 0±2‰ in marine carbonates). The δ¹³C in CP and LA are compatible with a dominant mantle carbon source. LTV and LH show lower (-10.72±0.46‰) and higher (-3.50±0.91‰) δ¹³C than the mantle values, respectively. Based on their helium (³He/⁴He) and carbon (δ¹³C) isotopic compositions, the variability of δ¹³C can be interpreted as caused by the (addition/mixing) of carbon organic matter-rich sediments from ancient subducting plates in LTV and from leaching of marine carbonates located underneath the basement in LH. The isotopic variability of oxygen is related to the extent of isotopic re-equilibration between steam (H₂O) and CO₂,

which in the case of fluids extracted from production wells may have not reached a full re-equilibration.

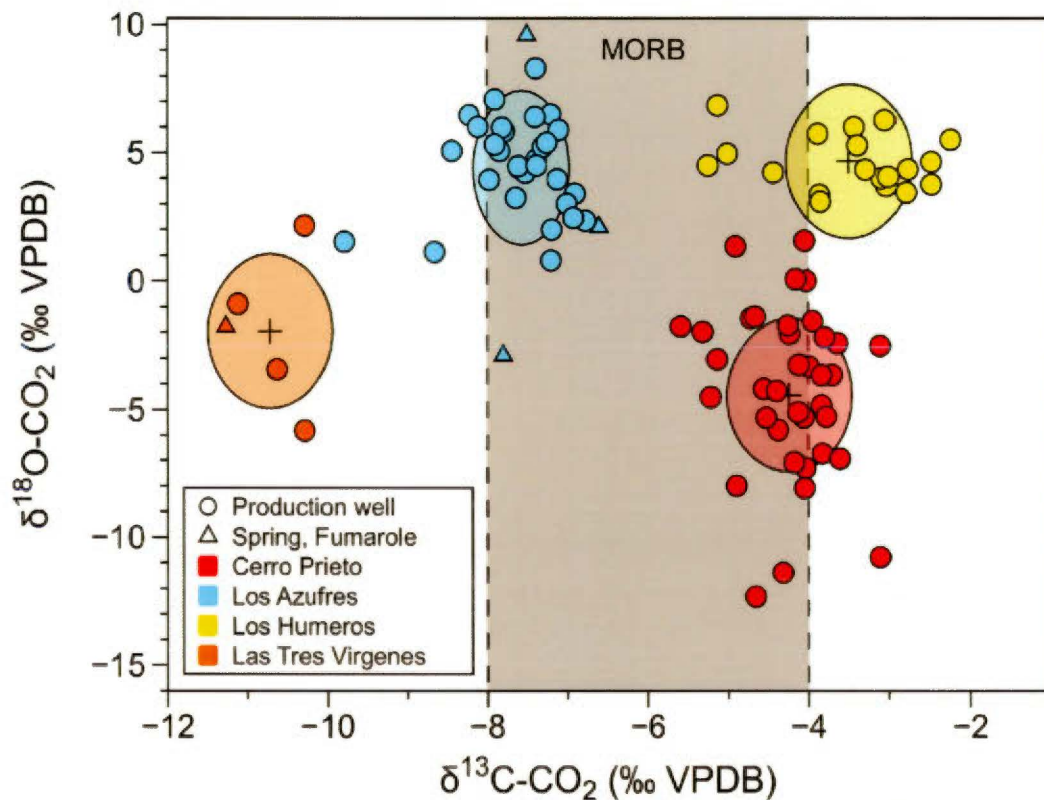


Figure 2.0. Graphical abstract. Distinct isotopic composition of carbon and oxygen in CO_2 from production wells, hot springs and fumaroles of Mexican geothermal fields. The values in each field is discretely highlighted by ellipsoids of different colors which represents the total method variability around a mean value which is represented by the cross sign.

2.1 Introduction

It is only in the last few years that scientists have sought to deepen their knowledge on the quantities, movements, forms, and origins of the so-called “deep carbon” (Dasgupta and Hirschmann, 2010). Although it is widely known that mantle carbon through volcanism has triggered some of the more drastic climate changes over geologic times and biological crisis (Hoffman et al., 1998; Zachos et al., 2005), there is a lack in the understanding of deep geological carbon cycle (Sano and Williams, 1996).

Basically, carbon is assumed to degas from mid-ocean ridges (Marty and Jambon, 1987) and in back-arc basins (Lan et al., 2010) into the atmosphere and be recycled through subduction either as sedimentary carbon (Sano and Williams, 1996) or possibly marine carbonates (Mason et al., 2017). Only a small fraction of sedimentary carbon is subducted (Kelemen and Manning, 2015), the majority is re-emitted into the atmosphere through arc volcanism (Sano and Williams, 1996). If this basic model of carbon cycling is widely accepted, yet the fluxes of carbon in and out the interior of the Earth and the sources of carbon in the different reservoirs need to be clarified. As an example, based on a compilation of published C ($\delta^{13}\text{C}$) and He (${}^3\text{He}/{}^4\text{He}$ ratios) isotopic data, Mason et al. (2017) have shown that carbon isotope composition of mean global volcanic gas is considerably higher, -3.8 to -4.6 per mil (‰), than the canonical mid-ocean ridge basalt value of $-6.0 \pm 2\text{‰}$ (e.g., Javoy et al., 1986). The largest volcanic emitters of carbon with higher $\delta^{13}\text{C}$ are located in mature continental

arcs that have accreted carbonate platforms, indicating that reworking of crustal limestone is an important source of volcanic carbon (Mason et al., 2017), not of organic carbon as previously postulated (Aiuppa et al., 2017). The fate of this sedimentary carbon back to mantle, is also a focus of much debate in the community of diamonds. The “eclogitic diamonds”, showing C isotopic compositions as low as -25‰ (Cartigny, 2005), are believed to indicate recycling of organic C into the mantle participating to the formation of these gems. But recent work of Bureau et al. (2018) has shown that lithospheric monocrystalline, fibrous and coated diamonds grow from a unique carbonate-rich fluid. Isotopic variability in diamonds might be related to different redox conditions during the crystal growth rather than to the variability in carbon sources (Bureau et al., 2018).

These few examples highlight the importance to study the behavior and identify carbon sources from the different Earth's reservoirs. Geothermal areas are important regions at the interface between the continental crust and the subcontinental mantle. Geothermal fluids, at temperatures up to 400°C, are fluids of complex nature (Yardley and Bodnar, 2014) with specific isotopic fingerprints (e.g., helium and carbon isotopes) of the interactions between the crust and the mantle. CO₂ is the natural dominant molecule of the dry volatile phase in geothermal fluids, often accounting for more than 90% of the total volume of gases (e.g., Tabaco et al., 1991; Birkle et al., 2001; Verma et al., 2006). Studying carbon sources in geothermal

aqueous fluids is therefore a mean to better understand the interactions between the crust and the mantle and the fate of C in these reservoirs.

This study aims to evaluate the C sources and its behavior in geothermal fluids. We therefore study the CO₂ stable isotopic composition ($\delta^{18}\text{O}$ - and $\delta^{13}\text{C}$ -CO₂; $^{18}\text{O}/^{16}\text{O}$ in geothermal CO₂ has been rarely analyzed) in fluids from the four major Mexican geothermal fields actually exploited for electricity production by the Comisión Federal de Electricidad (CFE) of Mexico. The extensive sampling campaign has been conducted between 2014 and 2016 at Cerro Prieto (CP), Los Azufres (LA), Los Humeros (LH) and Las Tres Vírgenes (LTV) fields (Fig. 2.1). To better constrain the carbon nature in these fields, isotopic data measured from the CO₂ molecule ($\delta^{18}\text{O}$ and $\delta^{13}\text{C}$) in this study have been compared to those of the water ($\delta^{18}\text{O}$) and helium isotopic ratio ($^3\text{He}/^4\text{He}$) obtained in the same campaign and published elsewhere (Pinti et al., 2017; Pinti et al., 2018; Nuñez-Hernández et al., 2018; Wen et al., 2018) and from a previous sampling campaign at Los Azufres done between 2007 and 2009 (Pinti et al., 2013).

2.2 Geology, hydrology and geochemistry of the studied fields

The geology of the four geothermal fields (GFs) exploited by the CFE in Mexico have been here classified based on the new “geothermal play type” concept proposed by Moeck and Beardmore (2014). A “play type” in geothermal resources is defined by the heat source, the geological controls on heat transport and thermal

energy storage capacity (Moeck and Beardsmore, 2014). The four studied geothermal fields are known as convection-dominated geothermal plays, which include all known ‘high temperature’ ($>200^{\circ}\text{C}$) geothermal reservoirs shallower than 3,000 m. These fields invariably lie on adjacent margins to tectonic plates or on regions of active tectonism, active volcanism, young plutonism, and elevated heat flow due to crustal thinning during extensional tectonics (Moeck and Beardsmore, 2014). In convection-dominated geothermal plays, heat is transported efficiently from deeper places to shallower reservoirs by the upward movement of fluid along permeable pathways. Convection-dominated geothermal plays can be further divided by the nature of the heat source. The LA-GF and LH-GF are known as extrusive magmatic plays which are distinguished by a shallow and intense heat source in the form of a young magma chamber (generally less than 100 kyr; e.g., Hayba and Ingebritsen, 1997) related to a magmatic arc above a subduction zone in convergent plate margins. The CP-GF and LTV-GF belong to extensional domain geothermal plays where the heat flow is elevated due to crustal extension and thinning.

2.2.1 The Cerro Prieto Geothermal Field (CP-GF)

The CP-GF is located in the Baja California (Fig. 2.1), about 30 km south of the town of Mexicali. It is the largest high-enthalpy ($> 280^{\circ}\text{C}$) compressed liquid-dominated geothermal system in Mexico. In the last 50 years, 429 geothermal wells were drilled in CP-GF at depths varying between 1,000 and 4,400 meters. Currently,

147 operating wells extract approximately 34.6 million metric tons of steam per year (Gutiérrez-Negrín, 2015).

The CP reservoir is part of a pull-apart basin formed by the active strike-slip Imperial Fault in the northeast and Cerro Prieto Fault in the southwest of the field, both belonging to the San Andreas Fault System (Suárez-Vidal et al., 2008). The heat source of the field is gabbro intruded less than 100 kyrs ago as a stress response of the extensional crustal thinning (Elders et al., 1984; Schmitt et al., 2013). The basement of the field is mainly composed of Cretaceous granites. On top of it rests a sequence of Plio-Pleistocene sedimentary rocks (Colorado River sandstones interbedded with gray shales called “Lutita Gris”) with a mean thickness of 2,400 meters and porosities of up to 22 % hosts the geothermal reservoir. The Lutitas Gris formation is overlain by brown shales (Lutita Café) and mudstones which act as the regional caprock. The unconsolidated quaternary clastic sediments of the Colorado River lie at the top of the stratigraphic sequence (Herrera, 2005).

The natural recharge of the geothermal field is likely assured by the shallow regional aquifer (Truesdell et al., 1979; Pinti et al., 2018). The reservoir temperature ranges from 250 to 310°C. Water is of sodium chloride type with neutral to alkaline pH (Gutiérrez-Negrín, 2015). The CO₂ represent 78-91% (m/m) of average dry gas fraction (Nehring and D'Amore, 1984). The C isotopic composition of the CO₂ from the first drilled wells, which are mostly abandoned, showed a range of $\delta^{13}\text{C}$ from -6.9 to -4.9‰ (Truesdell et al., 1979; Janik et al., 1982).

2.2.2 Los Azufres Geothermal Field (LA-GF)

The LA-GF is located in the Trans-Mexican Volcanic Belt (TMVB; Fig. 2.1) about 80 km east of Morelia in the central Michoacan State. It is the second geothermal field in Mexico for energy production, with a production area of 35 km² located at an average elevation of 2800 masl (Gutiérrez-Negrín, 2015). Most of its geothermal activity is concentrated in the southern portion of a sierra filled with Miocene andesites and Quaternary dacites, rhyolites and basalts. The southern portion is divided geographically into two zones: the Northern Production Zone (NPZ) and the Southern Production Zone (SPZ). The NPZ is in the compressed liquid region, and the SPZ has different systems depending on depth, which changes to the vapor-dominated, liquid-dominated and compressed-liquid regions as the depth becomes shallow (Torres-Rodríguez et al., 2005).

The geothermal reservoir is hosted in a 2700 m-thick fractured volcanic rocks, which is constructed by Upper Miocene to Pliocene (18.1-5.9 Ma) basaltic andesite to dacite complex, called the Mil Cumbres andesite (Dobson and Mahood, 1985). The reservoir is overlain by Quaternary (0.87 – 0.85 Ma) andesitic lavas and basaltic andesites of the Zinapecuaro unit that acts as a cap-rocks of a silicic sequence of rhyodacites, rhyolites, and dacites with ages ranging from 1.6 Ma and 15,000 years (Pérez et al., 2010). The heat source of the field is of unclear origin. On the basis of helium and strontium isotopic data, Wen et al. (2018) recently suggested that a MORB-like (Middle Ocean Ridge basalts) parental magma, possibly the one which

produced the La Calabaza and Llano Grande mafic lava flow sequences younger than 0.6 Ma (Pradal and Robin, 1994), could be the main heat source of the geothermal field.

The LA-GF is associated with a highly fractured geothermal reservoir, with faults in three directions; E-W, NE-SW, and NNW-SSE. The production wells were often drilled at the intersection of these two fault systems, in order to encounter higher reservoir permeability. The reservoir has a temperature range of 240 to 320 °C and is naturally recharged by the shallow regional aquifer and local precipitations (Torres-Rodríguez et al., 2005). The water fraction is of sodium chloride type with pH values between 5.8 and 7.2 (Birkle et al., 2001). CO₂ constitutes the 94% of the average dry gas fraction (Gutiérrez-Negrín, 2015). A few $\delta^{13}\text{C}$ -CO₂ measurements were obtained from production wells and yielded values ranging from -16.1‰ to -5.4‰ (Tabaco et al., 1991; Birkle et al., 2001; Pinti et al., 2013).

2.2.3 Los Humeros Geothermal Field (LH-GF)

The LH-GF is located on the eastern portion of the Plio-Pleistocene Trans-Mexican Volcanic Belt (Fig. 2.1), near the border with the Sierra Madre Oriental province. The field is located inside a twofold nested caldera complex produced by several rhyodacitic-andesitic plinian eruptions that started during the Miocene and lasted until 20 ka ago. The external Los Humeros Caldera is the oldest (460 ka) and the largest, with a diameter of 15-20 km. The internal Los Potreros Caldera is the

youngest (100 ka) and has a diameter of 8-10 km (e.g., Norini et al., 2015) and is the location of an active geothermal field that covers 17 km² at surface. The heat source of the field is a magmatic chamber at the terminal hydrothermal stage (Gutiérrez-Negrín et al., 2010).

The geothermal reservoir of the Los Humeros system consists of a sequence of blocks delimited by faults arranged as graben and horst and associated with the collapse of the Los Humeros Caldera formation. The LH-GF stratigraphy is composed of four geological units, from bottom to top: Unit (4) is the basement with granites and schists of Paleozoic age, covered by a thick series of Jurassic and Cretaceous limestones, metamorphosed during the Laramide orogeny and by Oligocene magmatic intrusions (De la Cruz, 1983). Unit (3) consist of Mio-Pliocene (10-1.9 Ma) pre-caldera volcanic deposits represented by the Teziutlán and Alseseca andesites intercalated with tuff horizons. Unit (2) is composed of Quaternary caldera volcanic products (510 ka – 100 ka) namely the Zaragosa and the Xaltipan andesites. Unit 1 consists of Quaternary rocks (<100 ka) related to the collapse of Los Potreros Caldera.

Recharge might occur locally, from rainfall infiltrating the reservoir through fault and fracture systems (Cedillo Rodríguez, 2000) bordering the Los Proteros escarpment (Pinti et al., 2017). The reservoir has a temperature of 210 to 380 °C (Gutiérrez-Negrín, 2015) and contains fluids of sodium chloride to bicarbonate-sulfate type with a neutral pH (Arellano et al., 2003). However, very acidic fluids

($\text{pH} < 4.5$) were found in the center of the field, possibly related to condensation of superheated steam containing HCl (Bischoff et al., 1996). The average dry gas fraction of the geothermal fluids contains up to 96% of CO₂ (González-Partida et al., 1993). Carbon of the CO₂ molecule has been studied by González-Partida et al. (1993) and Portugal et al. (1994, 2002) who reports $\delta^{13}\text{C}$ -CO₂ values from -6.6 to -3.2‰.

2.2.4 Las Tres Vírgenes Geothermal Field (LTV-GF)

LTV-GF is located in the northern portion of Baja California Sur (Fig. 2.1). The LTV-GF is located in a NW-SE oriented Plio-Quaternary rift called Santa Rosalía Basin (López et al., 1995). This basin constitutes the western limit of the deformation zone related to the opening of the Gulf of California, which created several young oceanic basins inter-connected by transform faults (Fig. 2.1; Arango-Galván et al., 2015). This area was, during the Miocene, the subduction zone of the Farallon plate under the American continent (Comondú arc in Fig. 2.1; Aguillón-Robles et al., 2001; Bellon et al., 2006; Calmus et al., 2008; Ferrari et al., 2012). The field is located within three volcanic eruptive centers: La Reforma caldera (3.5 to 0.8 Ma), Sierra de Aguajito (0.7-0.45 Ma) and Las Tres Vírgenes complex (0.44 Ma- 30 ka) (López et al., 1995; Schmitt et al., 2010).

The majority of the thermal activity is located at the border of the Las Tres Vírgenes volcanic complex with the El Aguajito Caldera, where geophysical prospecting

indicates the presence of conductive bodies at depths of 1.5 to 12 km (Prol-Ledesma et al., 2016). The reservoir is located in the basement and corresponds to low-permeability Upper Cretaceous granodiorites (Hinojosa et al., 2005). The basement is overlain by 750 m of Upper Oligocene to Middle Miocene volcano-sedimentary sandstones and andesites (Santa Lucía Fm) of the Comondú group (López et al., 1995; Macías Vázquez and Jiménez Salgado, 2013) which may behave as caprock. Over the Comondú group rests the Late Miocene Esperanza Formation initially described as tholeiitic basalts but now considered to be the product of subduction and to be similar to adakites (e.g., Aguillón-Robles et al., 2001; Calmus et al., 2011). These basalts are overlain by 300 m of sands, conglomerates and pyroclastics, which were deposited in the shallow marine environment of the Pliocene to Quaternary depression of the Santa Rosalía Basin (López et al., 1995).

Recent studies have shown that the most permeable zone of the LTV reservoir has a thickness of approximately 300 m and that the exploitable area is about 6 km² (Tello-López and Torres-Rodríguez, 2015). The shallow regional aquifer acts as the natural recharge of the reservoir, which has a temperature ranging from 250 to 275 °C (Tello-López and Torres-Rodríguez, 2015). The water fraction is of sodium chloride to bicarbonate-sulfate type (Barragán et al., 2010) with a neutral pH. CO₂ represents 97 to 99 wt% of the average dry gas fraction (Verma et al., 2006). Only a single $\delta^{13}\text{C}$ of CO₂ value of -10.1‰ has been reported in literature (Birkle et al., 2016).

2.3 Sampling and analytical methods

2.3.1 Sampling

To obtain a substantial database on the carbon dioxide of geothermal fluids, an exhaustive sampling campaign was carried out between 2014 and 2016 in the framework of the CeMieGEO (Centro Mexicano de Innovación en Energía Geotérmica) Project 20. LA-GF has been sampled in November 2014; LH-GF sampling campaign has been conducted in January 2015, while CP-GF and LTV-GF have been sampled in November 2016. A dataset on the isotopic composition of CO₂ from gas samples collected in 2007-2009 by Pinti et al. (2013) has been corrected and included in this study. A total of 105 sites have been sampled for gas phase. Among these samples, 96 contained enough CO₂ to be analyzed for δ¹⁸O-CO₂ and δ¹³C-CO₂, while 141 water samples were analyzed for the stable isotopic composition of water and mainly published elsewhere (Pinti et al., 2013; Pinti et al., 2017; Nuñez-Hernández et al., 2018).

Gas and water samples were collected using a similar method to the one described in Pinti et al. (2017). Gas samples were collected on the wellhead after the steam-water “Webre” separator (Fig. 2.2; Point A). At one of the valve manifolds along the steam tube (used for collecting purposes), a refrigeration-grade 3/8" copper tube was connected, using NPT-type female connector for airtightness purpose. The internal pressure of the steam tube was maintained slightly higher than the

atmospheric pressure, allowing the purge of the air present in the tube and avoiding air contamination. The gas circulates through the copper tube for several minutes until a constant outgoing flow was obtained. The $\sim 14 \text{ cm}^3$ gas aliquot was then hermetically sealed using stainless-steel pinch-off clamps closed using an electric driller (Pinti et al., 2017). Hot springs and fumaroles were sampled using a plastic funnel connected to the copper tube sampling systems using an armored 3/8" PVC tube. The fumarole gas pressure is equal or lower than atmospheric pressure and thus at the end of the copper tube a PVC tube is connected and plunged into a bottle of water, to avoid air entering from the back of the sampling system. Water samples are always taken at the weirbox at the exit of the silencer using a metal vessel (Fig. 2.2; Point B). Water is then rapidly transferred to 1-L Nalgene bottles which were washed previously with the same discarded geothermal water. LTV-GF is known to have carbonate-scaling problems (Flores-Armenta and Jaimes-Maldonado, 2001). Therefore, an inhibitor is usually injected by CFE to prevent obstruction of the wells such as LV-6 well. To verify whether inhibitor chemicals could have an effect on the carbon isotopic composition, a water sample from LV-6 well has been taken during the normal injection of inhibitor and after a 24-hour injection cessation. No significant changes on the $\delta^{13}\text{C}-\text{CO}_2$ has been observed between the two samples within analytical uncertainty.

2.3.2 Analytical methods

Geothermal gas samples contain others incondensable gases (e.g. H₂S, CH₄, N₂, Ar, Ne, He) and often condensate water that need to be separated from the CO₂ for isotopic analysis of CO₂. In laboratory, the first step is to extract the gas from the sample. In the following purification phase, a cryogenic separation is needed to remove the remnant water and the incondensable gases. A cryogenic liquid nitrogen and isopropyl dry ice mix method (Keeling, 1958) is used to recover a maximum of CO₂. After recovering a variable amount of CO₂ gas in a Pyrex glass vessel, isotopic composition of C and O were determined at the Geotop research center of Université du Québec à Montréal using an Isoprime 100 Dual Inlet Isotope Ratio Mass Spectrometer (IRMS). The samples were compared to a working CO₂ standard that has been normalized to the V-PDB scale using CO₂ evolved by the acidification of (at 25°C) LSVEC and NBS19 reference material as two anchors points (Coplen, 2006). The results are reported on the VPDB-LSVEC scale using the delta notation.

2.3.3 Assessment of the total method variability

To ensure that the sampling method produced reproducible isotopic analyses, a CO₂ stable isotope variability assessment was carried out, on steps from sampling through analysis. For this purpose, two wells were chosen for their different depths and position at the CP-GF. The CP-302 well is the second shallowest well in the field with a depth of 1324 m. The CP-346 well is one of the two deepest wells together

with CP-542, which are at an equal depth of 4000 m. Both wells have been sampled five times for CO₂ isotopic measurements using the same sampling methodology. Each sample was analyzed twice for its δ¹³C-CO₂ and δ¹⁸O-CO₂ composition. Although a minimum of three samples is commonly used to assess the variability of a method, a maximum of only two analyses was possible due to the volume of the sampling tube. The highest variabilities from the δ¹³C-CO₂ and δ¹⁸O-CO₂ measured in the same tube are respectively of ± 0.6 and ± 0.5 ‰ (Table 2.A.1; Appendix). However, if results for all of the five samples from the same well are taken, then the variability increases to ± 0.8 ‰ and ± 3.0 ‰ for the δ¹³C-CO₂ and δ¹⁸O-CO₂ respectively. The extraction, purification and analysis are assumed to induce the smallest variability, while the sampling may account for the rest of the variability measured from the five samples of the same well.

The sample internal pressure, which was determined in the laboratory, is plotted against the CO₂ isotopic composition for samples from CP-GF and LTV-GF (see Figure 2.A.1 in Appendix and Table 2.A.1). Only part of the samples we obtained during the 2014-2016 campaigns is shown in Figure 2.A.1, because accurate pressure measurements were possible only late during the measurements. A linear regression between sample internal pressure and the δ¹⁸O-CO₂ is calculated for the CP-GF samples. A minimum threshold of 2 bar is observed from the regression (Fig. 2.A.1). This threshold may reflect the lower amount of CO₂ that probably approaches the limit of detection of the IRMS. The resulting equation and coefficient of

determination (R^2) are 2748.7 - 193.91(x) and 0.78 respectively. No correlation can be observed between the sample internal pressure and the $\delta^{13}\text{C-CO}_2$ values (Fig. 2.A.1). Thus, it indicates that the $\delta^{18}\text{O-CO}_2$ may be fractionated in function of the fluid pressure flowing through the copper tube. Therefore, for further geothermal gas sampling, we propose to close the downstream pinch-off clamp and let the sample equilibrated with the production line for 5 minutes. This would prevent any fractionation of $\delta^{18}\text{O-CO}_2$ caused by pressure variation relative to the production well.

To fully understand the source of the oxygen fractionation, we also measured the $\delta^{18}\text{O}$ of condensate water from a gas sample and compared it to the $\delta^{18}\text{O-CO}_2$. We consistently obtained values that are coherent with equilibrium between the two molecules at the laboratory temperature (Table 2.A.2). Therefore, the $\delta^{18}\text{O-CO}_2$ variability might have been also caused by partial re-equilibrium between CO_2 and water at low temperature.

2.4 Results

The geothermal field sampled, the type of fluid collected, the year of sampling, $\delta^{13}\text{C-CO}_2$ and $\delta^{18}\text{O-CO}_2$ (with their analytical uncertainties) are reported in Table 2.1. The CO_2 stable isotopic compositions are reported using the delta notation in per mil (e.g., $\delta^{13}\text{C} = (^{13}\text{C}/^{12}\text{C})_{\text{sample}}/(^{13}\text{C}/^{12}\text{C})_{\text{std}} - 1 \times 1000$) and against VPDB (Coplen, 2011).

Figure 2.3 reports the $\delta^{13}\text{C-CO}_2$ vs $\delta^{18}\text{O-CO}_2$ values measured in production wells, hot springs and in fumaroles, where the values in each field is discretely highlighted by ellipsoids of different colors which represents the total method variability around a mean value which is represented by the cross sign. Except for a few outliers, each sampled geothermal field has a unique and distinct isotopic signature of C and O of the CO_2 molecule. In this figure and in the following one, Los Azufres results from this study and from Pinti et al. (2013) will be considered as a whole. The CP-GF samples show CO_2 with a $\delta^{13}\text{C-CO}_2$ ranging from -5.59 to -3.11‰ (median value of -4.13‰) and $\delta^{18}\text{O-CO}_2$ from -12.32 to +1.57‰ (median value of -4.2‰). The LA-GF fluids contain C with a $\delta^{13}\text{C-CO}_2$ ranging from -9.79 to -6.60‰ (median value of -7.51‰) and oxygen with a $\delta^{18}\text{O-CO}_2$ from -2.90 to +9.60‰ (median value of +4.62‰). The isotopic composition of CO_2 in the CP-GF and LA-GF falls mainly inside the canonical mantle $\delta^{13}\text{C}$ value range of $-6 \pm 2\text{\textperthousand}$ (Javoy et al., 1986; Mason et al., 2017). Los Humeros CO_2 shows $\delta^{13}\text{C-CO}_2$ ranging from -5.25 to -2.24‰ (median value of -3.29‰) and $\delta^{18}\text{O-CO}_2$ from +3.09 to +6.85‰ (median value of +4.42‰). LTV-GF fluids shows a restricted range of $\delta^{13}\text{C-CO}_2$ ranging from

-11.27 to -10.28‰ (median value of -10.63‰) and oxygen with a $\delta^{18}\text{O}$ -CO₂ from -5.82 to +2.16‰ (median value of -1.78‰) (Fig. 2.3; Table 2.1). The C isotopic composition of LTV-GF and LH-GF fluids show thus deviations from the C mantle value of -6 ±2‰, with lower and higher isotopic compositions, respectively.

In Figure 2.4 the $\delta^{13}\text{C}$ -CO₂ values measured in the four geothermal fields of this study are compared to values reported in the literature, often during the first phases of activity of the field (Birkle et al., 2001; Birkle et al., 2006; González-Partida et al., 1993; Janik et al., 1982; Portugal et al., 2002; Portugal et al., 1994; Tabaco et al., 1991; Truesdell et al., 1979). We can notice that except for LA-GF and LTV-GF, most of the measured C isotopic composition are within the canonical values of mantle C (-6±2‰; Javoy et al., 1986), indicating that this is the main source of carbon in the fields. It can be observed that CP-GF and LH-GF have a CO₂ carbon isotopic composition slightly higher than those measured previously in these fields. This could be caused by the continuous exploitation of the fields and boiling processes, being ¹³C preferentially fractionated in the steam phase (Tabaco et al., 1991). However, the difference between initial values and those after 30-50 years of exploitation differ by less than 1.5‰ (Fig. 2.4), except for LA-GF. Here, a notable difference is observed where depleted C values down to -16.1‰ are reported in the literature (Birkle et al., 2001). However, the median value of the previous dataset of Birkle et al. (2001) is -8.1‰ which is close to the median value of -7.5‰ of our dataset. These few lower values could indicate organic contamination of the samples

or that sedimentary C could have mixed with the dominant magmatic C component (Tabaco et al., 1991).

2.5 Discussion

2.5.1 Inter-field C and O isotopic variability

In Figure 2.3, variations of $\delta^{13}\text{C}$ values are expected to be controlled by terrestrial C sources (mantle, carbonate and organic matter (sedimentary) carbon) and/or reactions with carbonates at lower temperatures (e.g., Tabaco et al., 1991; Mook et al., 1974; Javoy et al., 1986; Sano and Marty, 1995).

The $\delta^{18}\text{O}$ should be controlled principally by the ^{18}O exchange between steam and carbon dioxide (e.g., Chiodini et al., 2000), which extent depends on the temperature at which this exchange proceeds (e.g., Bottinga, 1969) and the initial ^{18}O composition of both water and CO_2 . A study of the $\delta^{18}\text{O}$ measured in fumaroles and hot springs in several volcano-hydrothermal systems by Chiodini et al. (2000) has shown that ^{18}O exchange between CO_2 and steam is fast enough in natural gas phases to allow rapid isotopic re-equilibration within a wide temperature range (100 –1000°C). As for most isotopic exchanges, the effect of fractionation decreases with increasing temperature, becoming practically negligible above the critical temperature of water (e.g., Bottinga, 1969; Richet et al., 1977). In the following two sections, both the O and the C isotopic variability among the studied fields will be discussed.

2.5.2 The O isotopic variability

Figure 2.5 shows $\delta^{18}\text{O}$ values of water in the studied GFs (data from Pinti et al., 2013; Pinti et al., 2017; Pinti et al., 2018; Nuñez-Hernández et al., 2018) plotted against the $\delta^{18}\text{O}$ values of CO_2 from this study and recalculated by normalizing against VSMOW (Eqn. 2). There is a rough general trend indicating that the oxygen stable isotopic composition of the two phases are related and thus partial or total re-equilibration between the two phases occurs. The large scattering around a linear trend could be caused by the overlapping of other processes at depth, such as ^{18}O exchange with silicates or carbonates (e.g., Clayton and Steiner, 1975; Hedenquist and Lowerstern, 1994). Most important for our discussion, this plot highlights the fact that each field has a distinct $\delta^{18}\text{O}$ signature of water, particularly for CP and LA (Fig. 2.5). This initial water composition can explain partially the $\delta^{18}\text{O}-\text{CO}_2$ distribution observed in Figure 2.3. Indeed, water from CP-GF is isotopically the lightest among the four fields with a median $\delta^{18}\text{O}-\text{H}_2\text{O}$ value of -7.38‰ while water from LA-GF is the heaviest, with a median $\delta^{18}\text{O}-\text{H}_2\text{O}$ value of -0.58‰. Since the equilibrium isotopic fractionation between ^{18}O of water and of CO_2 depends on the temperature and the initial ^{18}O -water composition, then the lower composition of water of CP-GF is likely to explain the lower $\delta^{18}\text{O}-\text{CO}_2$ composition observed in Figure 2.3, compared to that of LA-GF, LH-GF and LTV-GF which show intermediate $\delta^{18}\text{O}-\text{H}_2\text{O}$ median values of -3.19 and -2.97‰, respectively.

The initial $\delta^{18}\text{O-H}_2\text{O}$ value of the LTV-GF (Fig. 2.5) cannot solely explain the $\delta^{18}\text{O-CO}_2$ observed in the field (Fig. 2.3). Indeed, the median $\delta^{18}\text{O-H}_2\text{O}$ of LTV-GF is only 3‰ lower than that of LA-GF, yet the difference ($\Delta^{18}\text{O}$) of the final $\delta^{18}\text{O-CO}_2$ among the two fields is more than 7‰ (Fig. 2.3). This means that temperature differences between the two fields or incomplete re-equilibration of ^{18}O between the CO_2 and H_2O phase could occur, to explain the relatively low $\delta^{18}\text{O-CO}_2$ of LTV-GF (Fig. 2.2).

Chiodini et al. (2000), based on analyses of hot springs around the world, showed that the ^{18}O exchange between steam and carbon dioxide in volcanic and hydrothermal gases is very fast, and thus isotopic equilibrium are attained in a hydrothermal system. Figure 2.6 shows the equilibrium in the oxygen isotope exchanges between CO_2 and H_2O , represented by the “per mil fractionation” or “1000ln α ”, which is calculated as follows:

$$1000\ln\alpha(\text{CO}_2-\text{H}_2\text{O}) = 1000\ln[(1000+\delta^{18}\text{O-CO}_2)/(1000+\delta^{18}\text{O-H}_2\text{O})] \quad (1)$$

where the $\delta^{18}\text{O-CO}_2$ (vs VPDB; Table 2.1) can be recalculated on the VSMOW scale as follows:

$$\delta^{18}\text{O-CO}_2(\text{VSMOW}) = 30.92 + 1.03092 \times \delta^{18}\text{O-CO}_2(\text{VPDB}) \quad (2)$$

The per mil fractionation is plotted against the temperature of the isotopic equilibrium, here calculated as $1000/(T(\text{°C}) + 273.15\text{°C})$, i.e. the inverse of the

temperature in kelvins. Chiodini et al. (2000) obtained a relationship that can be represented by a third-order polynomial equation:

$$1000\ln\alpha(\text{CO}_2\text{-H}_2\text{O}) = -5.0103 + 19.271 \times (103/T) - 11.485 \times (103/T)^2 + 3.6664 \times (103/T)^3 \quad (3)$$

This equation slightly deviates from the theoretical one calculated by Richet et al. (1977) for the CO₂-H₂O system. In Figure 2.6, we simulated with boxes the range of per mil fractionation we should obtain for each field (based on the measured δ¹⁸O-CO₂ and δ¹⁸O-H₂O range values for each field) at the expected temperature ranges at the Webre separator. Because present-day separation temperatures were not available from CFE for each well, we used temperature ranges from literature for LA-GF (Barragán et al., 2005), LH-GF (Arellano et al., 2003), LTV-GF (Barragán et al., 2010) and CP-GF (Nieva et al., 1982). The per mil fractionation simulated at these temperatures are close to the expected equilibration. Shift from the full re-equilibration could be related to the initial δ¹⁸O-H₂O used. Indeed here we used measured values at the weirboxes, while these values should be corrected for fractionation produced when the total discharge fluid is separated between the liquid phases and vapor (e.g., Nieva et al., 1983; Barragán et al., 2005). Yet previous studies in those fields have shown that the differences between weirbox and separator δ¹⁸O-H₂O values are of the order of 0.5-2‰, yet insufficient to explain the deviation from the full equilibration for our samples. Partial re-equilibration of CO₂ and H₂O in the

copper tube samplers (Table 2.A.2) also cannot be excluded as a cause of the shift towards lower temperatures of re-equilibration in the diagram of Fig. 2.6, although a generalization of this phenomenon is difficult to demonstrate.

Finally, when we plot data from other fields, such as Larderello in Italy (Panichi et al., 1977), one can observe that full equilibration does not seem to be attained in geothermal wells. This suggests that the ^{18}O variability observed in CO_2 from the different fields can be explained by the partial ^{18}O exchange between steam and carbon dioxide at separation temperatures. These results indicate that the use of the $\text{CO}_2\text{-H}_2\text{O}$ geothermometer should be carefully evaluated when applied to geothermal well data (Panichi et al., 1977).

2.5.3 The C isotopic variability

Although the convective geothermal play (Moeck and Beardmore, 2014) indicates that the Mexican fields should have a strong magmatic component, the C isotopic composition should have a canonical upper mantle value of $-6 \pm 2 \text{ ‰}$ (Sano and Marty, 1995). Some physicochemical reactions (e.g. carbonate precipitation, crustal assimilation or contamination, CO_2 dissolution and equilibrium with CH_4) (Gilfillan et al., 2009; Güleç and Hilton, 2016; Mason et al., 2017; Roulleau et al., 2013) can induce shifts in the $\text{CO}_2\text{-C}$ isotopic composition.

The four distinct groups of isotopic compositions of CO_2 in Mexican fields (Fig. 2.3) can partly be explained by C sources and kinetics processes. The CP-GF

and LA-GF show $\delta^{13}\text{C}$ -CO₂ values which are within the mantle carbon canonical value of -6±2‰. Differences between the two fields will be discussed later in the discussion. However, the LH-GF shows $\delta^{13}\text{C}$ -CO₂ which shift towards higher values up to -2.24±0.02‰, while the LTV-GF is characterized by very low values down to -11.27±0.01 ‰.

The lower C isotopic compositions measured at LTV-GF can be explained by two different processes which will be investigate further: carbonate precipitation (calcium carbonate scale deposition), which is a major problem in this field (Ocampo-Díaz and Rojas-Bribiesca, 2004; Tello-López and Torres-Rodríguez, 2015); or mixing with an isotopically depleted source, i.e. organic matter in sediments (<-20‰) (e.g., Javoy et al., 1986; Sano and Marty, 1995; Barry et al., 2014; Paternoster et al., 2017).

The first hypothesis suggests carbon isotope fractionation associated with calcite precipitation (Hoefs, 2015), as possible process of ^{13}C depletion at LTV-GF. To model the amount of CO₂ that has to precipitate as carbonates to shift an initial mantle C (with $\delta^{13}\text{C}$ of -6 to -8‰; Fig. 2.3) to the average LTV-GF $\delta^{13}\text{C}$ -CO₂ value of -10.72 ‰, we used a simple open system fractionation equation (Gilfillan et al., 2009; Güleç and Hilton, 2016). The fractionation factor alpha (α) is determined using the relation developed by Bottinga (1969):

$$\begin{aligned}
 & 1000 \ln(\alpha) \delta^{13}\text{C}(\text{CaCO}_3\text{-CO}_2) \\
 & = \frac{-0.8910(10^9)}{T^3} + \frac{8.557(10^6)}{T^2} + \frac{-18.110(10^3)}{T} \\
 & + 8.270 \quad (4)
 \end{aligned}$$

Where the temperature T is calculated in kelvin units. Fractionation is assumed to follow a Rayleigh distillation (open system). The equation is then:

$$\delta^{13}\text{C-CO}_2\text{-measured} + 1000 = (\delta^{13}\text{C-CO}_2\text{-mantle} + 1000)f^{(\alpha-1)} \quad (5)$$

where f is the fraction of the residual CO₂ which did not undergo carbonate precipitation.

Results from Eqn. 5 suggest that 85-97% of the initial CO₂ in LTV-GF need to have undergone carbonate precipitation. The calculations were made considering an initial mantle value of -6‰ and well-head separation temperatures of 128-155°C; Barragan et al., 2010), which are well below the temperature range of LTV-GF reservoir (250-275°C; Tello-López et Torres-Rodríguez, 2015). Utilization of these values is supported by the fact that LTV-GF fluids becomes supersaturated in CaCO₃ below temperatures of ca. 200-150°C (Tello-López and Torres-Rodríguez, 2015). Scaling is likely produced when fluids rise and start to boil at lower temperatures than those in the reservoir (Ocampo-Díaz and Rojas-Bribiesca, 2004). If we assume the most depleted value for mantle C of -8‰, and the same well-head temperatures, then 67-88% of the initial amount of CO₂ is needed to reproduce the low δ¹³C composition

at LTV-GF fluids (Table 2.1; Fig. 2.3). Considering that the amount of CO₂ trapped by carbonates precipitation is commonly less than 25 % (Gilfillan et al., 2009; Güleç and Hilton, 2016), the extreme loss of CO₂ in the LTV-GF reservoir seems highly unlikely. Moreover, if carbonate precipitation occurs the CO₂/³He ratio should dramatically decrease from the initial value (Gilfillan et al., 2009), i.e. the mantle (2 x10⁹; Marty and Jambon, 1987). We did not measure CO₂ concentrations but in LTV CO₂ is relatively constant at 97-99 wt%. ³He contents range from 1.79 to 5.69 x 10⁻¹¹ cm³STP/cm³. The corresponding CO₂/³He ratios should range from 1.72 and 5.49 x 10¹⁰, which is higher than the mantle value, suggesting that carbonate precipitation is not a viable process to explain the lower δ¹³C composition of LTV CO₂. These estimated CO₂/³He ratios, together with the lower δ¹³C composition suggest a mixing with a ³He-depleted source such as organic C-rich sediments (Sano and Marty, 1995).

Modern contamination with organic matter have been discarded to explain low δ¹³C-CO₂ values considering that LTV-GF is actually an extremely arid area and thus recharge water is likely depleted in organic matter (Birkle et al., 2016). LTV-GF fluids are considered to be a mixture of late Pleistocene meteoritic water and of non-evaporated seawater (Birkle et al., 2016). Hence, paleo-organic contamination can be modelled with a simple mixing equation:

$$\delta^{13}\text{C-CO}_2\text{-total} = (x)(\delta^{13}\text{C-CO}_2\text{-OM}) + (-x)(\delta^{13}\text{C-CO}_2\text{-RW}) \quad (6)$$

where OM and RW are organic matter and recharge water, respectively.

Measurements of the $\delta^{13}\text{C}$ of the DOC (Dissolved Organic Carbon) in LTV-GF fluids (Pinti et al., 2018) show an average value of -27.8‰. Assuming this value for the organic matter and an average mantle $\delta^{13}\text{C-CO}_2$ of -6‰ (Javoy et al., 1986), then Eqn. 6 suggests a 21.6% contribution of carbon from organic matter and of 78.4 % of mantle carbon.

LTV-GF low $\delta^{13}\text{C-CO}_2$ values could derive from a contamination of organic matter-rich oceanic sediments during Tertiary paleo-subduction events. C-bearing molecules would mostly be organic-rich sediments accumulated on top of the slab. The LTV-GF is part of the Santa Rosalía basin which is known to contain adakites of 23 to 13 Ma ago, linked to the subduction of the Farallon plate that formed the Comondú volcanic arc (Fig. 2.1; Ferrari et al., 2012). Adakites are produced by the melting of subducted young oceanic crust at high thermal regime (Aguillón-Robles et al., 2001). Adakites are found all around the pacific ring of fire in subduction context, notably in the Aleutian and the Cascadia where $\delta^{13}\text{C-CO}_2$ values as low as at LTV-GF have been observed (Mason et al., 2017).

To confirm this hypothesis, proxies of sediment assimilation should be compared to the $\delta^{13}\text{C}$ values. One is the $\text{CO}_2/{}^3\text{He}$ ratio, which is compatible with a mixing between mantle and sedimentary C (the latter having a $\text{CO}_2/{}^3\text{He}$ of 10^{10} to 10^{12} ; O’Nions and Oxburgh, 1988). Another is the helium isotopic ratio ${}^3\text{He}/{}^4\text{He}$ (normally reported as R, and normalized to the atmospheric ratio $\text{Ra} = 1.384 \times 10^{-6}$;

Craig and Lupton et al., 1976). Indeed, high ${}^3\text{He}/{}^4\text{He}$ ratios are an indication of the presence of mantle fluids which are enriched in ${}^3\text{He}$, compared to ${}^4\text{He}$, with R/Ra values as high as 8 ± 1 in MORB sourced upper mantle (e.g., Graham, 2002). If there is sedimentary addition, the canonical upper mantle R/Ra value of 8 will be lowered by addition of radiogenic ${}^4\text{He}$ which is normally produced by U and Th decay in sediments (e.g., Pinti and Marty, 1998).

In Figure 2.7, the Rc/Ra values measured in the four geothermal fields (CP-GF, Pinti et al., 2018; LTV-GF, Pinti et al., 2018; LA-GF, Wen et al., 2018; LH-GF, Pinti et al., 2017) are plotted against the $\delta^{13}\text{C}-\text{CO}_2$ values measured in this study. Dashed lines are mixing hyperbolas (Langmuir et al., 1978) calculated for a mixture of mantle C and He ($\text{R/Ra} = 8\pm1$ and $\delta^{13}\text{C}-\text{CO}_2$ of $-6\pm2\text{\textperthousand}$) and two distinct sedimentary sources: organic matter-rich sediment ($\text{R/Ra} = 0.02$ and $\delta^{13}\text{C}-\text{CO}_2$ of -20 to $-25\text{\textperthousand}$; Sano and Marty, 1995) and carbonates ($\text{R/Ra} = 0.02$ and $\delta^{13}\text{C}-\text{CO}_2$ of -2 to $+2\text{\textperthousand}$; Pinti and Marty, 1998; Sano and Marty, 1995). The parameter “r” defines the degree of curvature between the two end-members, here the mantle and the two sedimentary sources. The helium and carbon signatures of the LTV-GF fluids is compatible with a mixing with organic-rich sediments, possibly to the addition of either slab- or crustal-derived carbon (e.g., Mason et al., 2017). Measured ${}^{87}\text{Sr}/{}^{86}\text{Sr}$ from LTV-GF fluids (0.7043, unpublished data) are consistent with either local granitic sources or subduction sediments (approx. 0.7045) (Thirlwall et al., 1996).

On the other hand, LH-GF fluids, which are characterized by $\delta^{13}\text{C}$ values slightly higher than the mantle carbon value (Fig. 2.3) may have undergone carbonate dissolution of the meta-carbonates composing the basement of the reservoir (Fig. 2.7), as suggested by González-Partida et al. (1993) and Peiffer et al. (2018). The occurrence of $^{87}\text{Sr}/^{86}\text{Sr}$ ratios higher than 0.709 measured in the fluids (Pinti et al., 2017) supports this hypothesis. Isotopic fractionation does not occur when passing from solid carbonates to dissolved CO₂. Thus, a simple binary mixing equation such as Eqn. (6) can be used to model the interaction of carbonates with the geothermal fluids. Therefore, using in Eqn. (6) the canonical $\delta^{13}\text{C}$ value of marine carbonates of $0\pm2\text{\textperthousand}$ (Sano and Marty, 1995) and a canonical mantle $\delta^{13}\text{C}$ value of $-6\pm2\text{\textperthousand}$ (Javoy et al., 1986), the average LH-GF $\delta^{13}\text{C-CO}_2$ value of $-3.30\text{\textperthousand}$ requires a contribution of 35 to 47% of carbonate C into the geothermal fluids of Los Humeros.

It is interesting to note that LH-GF, LA-GF and CP-GF show initial $\delta^{13}\text{C-CO}_2$ compatible with a mantle source but different helium isotopic compositions which seems to not reflect the geodynamic context of each geothermal field. LA-GF contain a pure mantle C and He source as those sourcing the MORBs ($\delta^{13}\text{C} = -7.5\text{\textperthousand}$ and $\text{Rc/Ra} = 7.9$) mixed with a radiogenic helium source as observed in volcanic arcs ($\text{R/Ra} = 5.4 \pm 1.9$; Hilton et al., 2002). LH-GF fluids seem to have an initial $\delta^{13}\text{C}$ and Rc/Ra value compatible with MORB-like source. Now both fields are within the Trans-Mexican Volcanic Belt (Fig. 2.8) which is the surface expression of the subduction of the Cocos plate under central Mexico (Fig. 2.1; Peréz-Campo et al.,

2008). It would be expected that mantle He shows isotopic composition similar to volcanic arcs, which is characterized by a ${}^3\text{He}/{}^4\text{He}$ ratio lower than a pure upper mantle signature of $8\pm1\text{Ra}$ (Hilton et al., 2002). The difference could be explained by the particular geometry of the slab under central Mexico. The plate plunges into the mantle near Mexico City (Fig. 2.8) almost vertically, which may explain that LH, which is at the northern border of the TMVB could receive almost directly lithospheric mantle material feeding the field with mostly pure upper mantle volatiles, including CO₂ and He (Fig. 2.7). LA is slightly northern than Mexico City (about 200 km west) on the vertical of the slab edge. Here, volatiles from both the lithospheric mantle and the subducting slab could reach the field. The occurrence of a mostly pure He mantle signal in LA is in agreement with recent findings of Wen et al. (2018) which shows, on the basis of Sr isotopic composition of fluids that MORB-like melts are feeding the field with heat and volatiles.

Most intriguing is the signature of the CP-GF fluids, which shows a pure mantle C signature but contain helium exclusively with an isotopic signature typical of volcanic arcs rather than from the upper mantle sourcing the MORBs (Fig. 2.7). Now CP is within a pull-apart basin corresponding to a continental extension with MORB-like melts at its base (Schmitt et al., 2013) and MORB-like ${}^3\text{He}/{}^4\text{He}$ would be expected, though in the nearby Imperial Valley clear upper mantle helium isotopic signatures have been never found (Welhan et al., 1979; 1988). The apparent contradiction can be explained by the presence of large amount of radiogenic helium

accumulated in the fluids of Cerro Prieto, that mask the original mantle signature of the CP fluids (Pinti et al., 2018). Indeed, Pinti et al. (2018) have shown that Cerro Prieto reservoir could be fossil, exploiting local connate waters older of a few million years and having accumulated radiogenic ${}^4\text{He}$ produced in situ. The high Rc/Ra of 7.32 ± 0.07 measured in well 423 at Cerro Prieto (Fig. 2.7; Pinti et al., 2018) is an indication that a pure mantle signal is present at Cerro Prieto, but presently masked by local sources of radiogenic ${}^4\text{He}$, possibly formed in carbonate-matrix rich sediments which could explain the slightly heavier composition of carbon in CP fluids compared to canonical value of the mantle (Fig. 2.6).

2.6 Conclusions

The origin and behavior of deep carbon has been investigated in deep-conductive geothermal systems, which are privileged areas of the continental crust where mantle addition of volatiles takes place. The carbon ($\delta^{13}\text{C}$) and oxygen ($\delta^{18}\text{O}$) isotopic composition has been measured in the CO_2 molecule, the most abundant volatile species in these systems. The most interesting finding of this work is that each geothermal field has its own C and O isotopic signature. This distinct signature is the result of their own hydrodynamic situation and their geodynamic context.

The $\delta^{18}\text{O}-\text{CO}_2$ is controlled by the exchange between oxygen from the steam and that of the CO_2 molecule in the reservoir. The differences observed are mainly related to the initial $\delta^{18}\text{O}$ of the geothermal fluids which in turn depends from the

isotopic signature of the recharge water and its level of mixing with either magmatic or andesitic water, i.e the level of evolution of the hydrodynamic state of the field. The second parameter which control the ^{18}O exchange between CO_2 and H_2O is the temperature of the reservoir (i.e. indirectly its enthalpy). What has been noticed here is that in geothermal wells, on the contrary of lower-T springs and fumaroles, the isotopic exchange of ^{18}O seems not to be fully reached. These results are not surprising: isotopic exchange is a kinetic process and in geothermal wells where several tens of tons of steam is rapidly brought from depths of 3-4 km to surface, it is highly unlikely that a complete isotopic re-equilibration at the well-head can take place. Variability of C isotopic composition is mainly controlled by mixtures between different carbon sources (mantle, sedimentary-organic and carbonate) which reflect the geodynamic context of the sampled field and partially the hydrodynamic situation. This is the case of Cerro Prieto, where fossil geothermal fluids accumulating radiogenic ^4He are masking the real mantle signature of the field, which is expected to be similar to that of MORBs, being Cerro Prieto located in an extensional context of transform faulting.

In conclusion this work final aim was to contribute to the general understanding of the deep carbon cycle and exploring venues to use C as a tracer of volatile sources and water-rock interaction processes of CO_2 at high temperatures in geothermal areas. Yet, several questions are still open, such as the intra-field variability of CO_2 isotopic composition and why canonical mantle value has so large

range of variability ($\Delta^{13}\text{C}$ of 4‰) in geothermal fluids. Isotopic fractionation between carbon species as suggested by Tabaco et al. (1991) are unlikely. Mantle CO_2 is the dominant species (close to 100% in cases such as CP-GF and LA-GF) and fractionation at reservoir temperatures of 250 to 400°C is 1‰ or even less. Further work and coupling with other isotopic tracers of mantle volatiles than helium, i.e. Sr isotopes, could be useful to determine the causes of this variability.

2.7 Acknowledgments

Review of earlier version from C. Hillaire-Marcel and Y. Sano were highly appreciated. This work was partially funded by CeMieGEO P-20 project from the CONACYT (Convocatoria SENER-CONACyT 2013-01, N° de proyecto 207032) and NSERC Discovery Grant to DLP and LR. We wish to thank the staff of the CFE Residencia of Los Azufres, Los Humeros, Las Tres Vírgenes and Cerro Prieto for access to the production wells and data. The authors also thank Aurora María Estrada Murillo, Sandra Nuñez and Jonny Bahena Romero who participated in the fieldwork.

2.8 Appendix

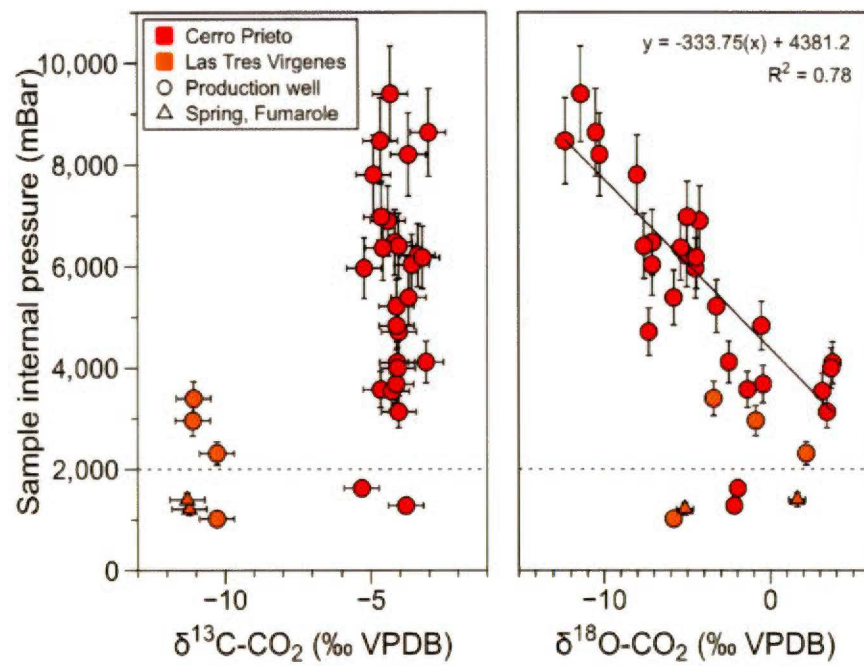


Figure 2.A.1. Sample internal pressure versus the CO_2 isotopic composition. The solid line is the linear correlation between the sample internal pressure and the $\delta^{18}\text{O}$ - CO_2 while the dash line represents the 2bar threshold.

Tableau 2.A.1. Repeated analyses of CO₂ isotopes in Cerro Prieto wells to test analytical consistency.

Name of well	$\delta^{13}\text{C-CO}_2$ (‰ VPDB)	±	$\delta^{18}\text{O-CO}_2$ (‰ VPDB)	±
CP-302 A	- 4.051	0.006	3.427	0.008
CP-302 B	- 4.282	0.006	3.139	0.007
CP-302 B	- 4.082	0.005	3.683	0.007
CP-302 C	- 4.098	0.005	3.763	0.006
CP-302 D	- 4.135	0.004	- 0.441	0.011
CP-302 D	- 3.880	0.004	0.516	0.008
CP-302 D	- 3.941	0.011	0.176	0.027
CP-302 D	- 3.894	0.003	0.431	0.010
CP-302 E	- 4.115	0.005	- 0.534	0.007
CP-346 A	- 3.713	0.004	- 10.257	0.012
CP-346 A	- 3.021	0.003	- 10.483	0.011
CP-346 C	- 3.393	0.005	- 5.039	0.010
CP-346 C	- 4.580	0.006	- 5.390	0.011
CP-346 D	- 3.708	0.008	- 5.809	0.014
CP-346 E	- 3.597	0.005	- 7.108	0.011
CP-346 F	- 3.233	0.003	- 4.477	0.005

Tableau 2.A.2. Measurements of oxygen isotopic signature in condensate water and steam from the same sampling tube.

Name of well	$\delta^{18}\text{O-H}_2\text{O}$ (‰ VPDB)	±	$\delta^{18}\text{O-CO}_2$ (‰ VPDB)	±	Equilibrium temperature (°C)*
	condensate		steam		
CP-112	-41.20	0.05	-1.45	0.01	26.98
CP-114	-42.10	0.05	-1.77	0.03	24.09
CP-301	-38.39	0.05	1.35	0.02	27.03
CP-302 A	-36.96	0.05	3.43	0.01	23.84
CP-308	-40.37	0.05	0.07	0.06	23.54

* Calculated following Bottinga (1968).

2.9 References

- Aiuppa, A., Fischer, T.P., Plank, T., Robidoux, P., Di Napoli, R., 2017. Along-arc, inter-arc and arc-to-arc variations in volcanic gas CO₂/ST ratios reveal dual source of carbon in arc volcanism. *Earth-Science Reviews* 168, 24-47.
- Aguillón-Robles, A., Calmus, T., Benoit, M., Bellon, H., Maury, R.C., Cotten, J., Bourgois, J., Michaud, F., 2001. Late Miocene adakites and Nb-enriched basalts from Vizcaino Peninsula, Mexico: Indicators of East Pacific Rise subduction below southern Baja California? *Geology* 29: 531-534.
- Arango-Galván, C., Prol-Ledesma, R.M., Torres-Vera, M.A., 2015. Geothermal prospects in the Baja California Peninsula. *Geothermics* 55: 39-57.
- Arellano, V., García, A., Barragán, R., Izquierdo, G., Aragón, A., Nieva, D., 2003. An updated conceptual model of the Los Humeros geothermal reservoir (Mexico). *J. Volcanol. Geotherm. Res.* 124: 67-88.
- Barragán, R.M., Arellano, V.M., Portugal, E., Sandoval, F., 2005. Isotopic ($\delta^{18}\text{O}$, δD) patterns in Los Azufres (Mexico) geothermal fluids related to reservoir exploitation. *Geothermics* 34: 527-547.
- Barragán, R.M., Iglesias, E.R., Arellano, V.M., Torres, R.J., Tapia, R., Hernández, P., Ramírez, M., 2010. Chemical modeling of fluids from the Las Tres Virgenes

BCS (México) geothermal field. Proc. World Geother. Congr., Bali, Indonesia, 25-29 April 2010, p.8.

Barry, P., Hilton, D., Füri, E., Halldórsson, S., Grönvold, K., 2014. Carbon isotope and abundance systematics of Icelandic geothermal gases, fluids and subglacial basalts with implications for mantle plume-related CO₂ fluxes. *Geochim. Cosmochim. Acta* 134: 74-99.

Bellon, H., Aguillón-Robles, A., Calmus, T., Maury, R.C., Bourgois, J., Cotten, J., 2006. La Purísima volcanic field, Baja California Sur (Mexico): Miocene to Quaternary volcanism related to subduction and opening of an asthenospheric window. *J. Volcanol. Geother. Res.* 152: 253-272.

Birkle, P., Merkel, B., Portugal, E., Torres-Alvarado, I.S., 2001. The origin of reservoir fluids in the geothermal field of Los Azufres, Mexico—isotopical and hydrological indications. *Appl. Geochem.* 16: 1595-1610.

Birkle, P., Marín, E.P., Pinti, D.L., Castro, M.C., 2016. Origin and evolution of geothermal fluids from Las Tres Virgenes and Cerro Prieto fields, Mexico—Co-genetic volcanic activity and paleoclimatic constraints. *Appl. Geochem.* 65: 36-53.

Bischoff, J.L., Rosenbauer, R.J., Fournier, R.O., 1996. The generation of HCl in the system $\text{CaCl}_2\text{-H}_2\text{O}$:Vapor-liquid relations from 380-500 °C. *Geochim. Cosmochim. Acta* 60: 7-16.

Bottinga, Y., 1968. Calculation of fractionation factors for carbon and oxygen isotopic exchange in the system calcite-carbon dioxide-water. *J. Phys. Chem.* 72: 800-808.

Bottinga, Y., 1969. Calculated fractionation factors for carbon and hydrogen isotope exchange in the system calcite-carbon dioxide-graphite-methane-hydrogen-water vapor. *Geochim. Cosmochim. Acta* 33: 49-64.

Bureau, H., Remusat, L., Esteve, I., Pinti D.L., Cartigny, P., 2018. The growth of lithospheric diamonds. *Sci. Adv.* 4: eaat1602.

Calmus, T., Pallares, C., Maury, R.C., Bellon, H., Pérez-Segura, E., Aguillón-Robles, A., Carreño, A.-L., Bourgois, J., Cotten, J., Benoit, M., 2008. Petrologic diversity of Plio-Quaternary post-subduction volcanism in northwestern Mexico: An example from Isla San Esteban, Gulf of California. *Bull. Soc. Géol. France* 179: 465-481.

Calmus, T., Pallares, C., Maury, R.C., Aguillón-Robles, A., Bellon, H., Benoit, M., Michaud, F., 2011. Volcanic markers of the post-subduction evolution of Baja

California and Sonora, Mexico: Slab tearing versus lithospheric rupture of the Gulf of California. *Pure Appl. Geophys.* 168: 1303-1330.

Cartigny, P., 2005. Stable isotopes and the origin of diamond. *Elements* 1: 79-84.

Cedillo Rodríguez, F., 2000. Hydrogeologic model of the geothermal reservoirs from Los Humeros, Puebla, Mexico. *Proc. World Geother. Congr. 2000*, Kyushu - Tohoku, Japan, May 28-June 10, 2000, p. 6.

Chiodini, G., Allard, P., Caliro, S., Parello, F., 2000. ^{18}O exchange between steam and carbon dioxide in volcanic and hydrothermal gases: implications for the source of water. *Geochim. Cosmochim. Acta* 64: 2479-2488.

Clayton, R.N., Steiner, A., 1975. Oxygen isotope studies of the geothermal system at Wairakei, New Zealand. *Geochim. Cosmochim. Acta* 39: 1179-1186.

Coplen, T. B., Brand, W., Gehre, M., Groning, M., Meijer, H., Toman, B., Verkouteren, M., 2006. New Guidelines for d13C measurements. *Anal. Chem.* 78: 2439-2441.

Coplen, T. B., 2011. Guidelines and recommended terms for expression of stable-isotope-ratio and gas-ratio measurement results. *Rapid Commun. Mass Spectrom.* 25:2538-2560.

Craig, H., Lupton, J., 1976. Primordial neon, helium, and hydrogen in oceanic basalts. *Earth Planet. Sci. Lett.* 31: 369-385.

Dasgupta, R., Hirschmann, M.M., 2010. The deep carbon cycle and melting in Earth's interior. *Earth Planet. Sci. Lett.*, 298: 1-13.

De la Cruz, M.P., 1983. Estudio geológico a detalles de la zona geotérmica de Los Humeros, Pue. CFE internal Report.

Dobson, P.F., Mahood, G.A., 1985. Volcanic stratigraphy of the Los Azufres geothermal area, Mexico. *J. Volcanol. Geotherm. Res.* 25: 273-287.

Elders, W., Bird, D., Williams, A., Schiffman, P., 1984. Hydrothermal flow regime and magmatic heat source of the Cerro Prieto geothermal system, Baja California, Mexico. *Geothermics* 13: 27-47.

Ferrari, L., Orozco-Esquivel, T., Manea, V., Manea, M., 2012. The dynamic history of the Trans-Mexican Volcanic Belt and the Mexico subduction zone. *Tectonophysics* 522-523: 122-149.

Flores-Armenta, M., Jaimes-Maldonado, G., 2001. The Las Tres Vírgenes Mexico geothermal reservoir. *Trans. Geother. Resou. Counc.* 25: 525-534.

Gillfillan, S.M., Lollar, B.S., Holland, G., Blagburn, D., Stevens, S., Schoell, M., Cassidy, M., Ding, Z., Zhou, Z., Lacrampe-Couloume, G., 2009. Solubility

trapping in formation water as dominant CO₂ sink in natural gas fields. *Nature* 458: 614-618.

González-Partida, E., Barragán, R., Nieva, D., 1993. Análisis geoquímico-isotópico de las especies carbónicas del fluido geotérmico de Los Humeros, Puebla, México. *Geof. Intern.* 32: 299-309.

Graham, D., 2002. Noble gases in MORB and OIB: observational constraints for the characterization of mantle source reservoirs. *Rev. Mineral. Geochem.* 47: 247-318.

Güleç, N., Hilton, D.R., 2016. Turkish geothermal fields as natural analogues of CO₂ storage sites: gas geochemistry and implications for CO₂ trapping mechanisms. *Geothermics* 64: 96-110.

Gutiérrez-Negrín, L.C., Izquierdo-Montalvo, G., Aragón-Aguilar, A., 2010. Review and update of the main features of the Los Humeros geothermal field, Mexico. *Proc. World Geother. Congr.* 2010, Bali, Indonesia, 25-29 April 2010, p.7.

Gutiérrez-Negrín, L.C., 2015. Mexican geothermal plays. *Proc. World Geother. Congr.* 2015, Melbourne, Australia, 19–25 April, p. 9.

Hayba, D.O., Ingebritsen, S.E., 1997. Multiphase groundwater flow near cooling plutons. *J. Geophys. Res.: Planets* 102: 12235–12252.

Hedenquist, J.W., Lowenstern, J.B., 1994. The role of magmas in the formation of hydrothermal ore deposits. *Nature* 370: 519-52.

Herrera, H.L., 2005. Actualización del modelo geológico conceptual del yacimiento geotérmico de Cerro Prieto, BC. *Géotermia* 18: 37-46.

Hilton, D.R., Fischer, T.P., Marty, B., 2002. Noble gases and volatile recycling at subduction zones. *Rev. Mineral. Geochem.* 47: 319-370.

Hinojosa, E.T., Verma, M.P., Partida, E.G., 2005. Geochemical characteristics of reservoir fluids in the Las Tres Virgenes, BCS, Mexico. *Proc. World Geother. Congr.* 2005 Antalya, Turkey, 24-29 April 2005, p. 11.

Hoefs, J., 2015. Stable isotope geochemistry. Springer-Verlag, 437 pp.

Hoffman, P.F., Kaufman, A.J., Halverson, G.P., Schrag, D.P., 1998. A Neoproterozoic snowball earth. *Science* 281: 1342-1346.

Janik, C., Nehring, N., Huebner, M., Truesdell, A., 1982. Carbon-13 variations in fluids from the Cerro Prieto geothermal system. *Proc. Fourth Symp. Cerro Prieto Geother. Field, Baja California, Mexico* 2: 535-541.

Javoy, M., Pineau, F., Delorme, H., 1986. Carbon and nitrogen isotopes in the mantle. *Chem. Geol.* 57: 41-62.

Keeling, C.D., 1958. The concentration and isotopic abundances of atmospheric carbon dioxide in rural areas. *Geochim. Cosmochim. Acta* 13: 322-334.

Kelemen, P.B., Manning, C.E., 2015. Reevaluating carbon fluxes in subduction zones, what goes down, mostly comes up. *Proc. Nat. Acad. Sci.* 112: E3997.

Lan, T.F., Sano, Y., Yang, T.F., Takahata, N., Shirai, K., Pinti, D.L., 2010. Evaluating Earth degassing in subduction zones by measuring helium fluxes from the ocean floor. *Earth Planet. Sci. Lett.* 298: 317-322.

Langmuir, C.H., Vocke Jr, R.D., Hanson, G.N., Hart, S.R., 1978. A general mixing equation with applications to Icelandic basalts. *Earth Planet. Sci. Lett.* 37: 380-392.

López, H., García, G., Arellano, F., 1995. Geothermal exploration at Las Tres Virgenes, BCS, Mexico. *Proc. World Geother. Congr 2005*, Florence, Italy, p. 707-712.

Marty, B., Jambon, A., 1987. C/He-3 in volatile fluxes from the solid Earth - Implications for carbon geodynamics. *Earth. Planet. Sci. Lett.* 83: 16-26.

Mason, E., Edmonds, M., Turchyn, A.V., 2017. Remobilization of crustal carbon may dominate volcanic arc emissions. *Science* 357: 290-294.

Moeck, I., Beardsmore, G., 2014. A new ‘geothermal play type’ catalog: Streamlining exploration decision making. Proc. Thirty-Ninth Workshop Geother. Res. Engin. Stanford Un., Stanford, California, February 24-26, 2014, SGP-TR-202, p.8.

Mook, W., Bommerson, J., Staverman, W., 1974. Carbon isotope fractionation between dissolved bicarbonate and gaseous carbon dioxide. Earth Planet. Sci. Lett. 22: 169-176.

Nehring, N., D'Amore, F., 1984. Gas chemistry and thermometry of the Cerro Prieto, Mexico, geothermal field. Geothermics 13: 75-89.

Nieva, D., Fausto, J., González, J., Garibaldi, F., 1982. Afluencia de vapor a la zona de alimentación de pozos de Cerro Prieto I. Fourth Symp. Cerro Prieto Geother. Field, Baja California, Mexico 2.

Nieva, D., Quijano, L., Garfias, A., Barragán, R.M., Laredo, F., 1983. Heterogeneity of the liquid phase, and vapour separation in Los Azufres (Mexico) geothermal reservoir. Ninth Workshop Geother. Res. Engin., Stanford Un., California, USA, pp. 253-260.

Norini, G., Groppelli, G., Sulpizio, R., Carrasco-Núñez, G., Dávila-Harris, P., Pellicioli, C., Zucca, F., De Franco, R., 2015. Structural analysis and thermal

remote sensing of the Los Humeros Volcanic Complex: Implications for volcano structure and geothermal exploration. *J. Volcanol. Geother. Res.* 301: 221-237.

Nuñez-Hernández, S., Pinti, D.L., López-Hernández, A., Shouakar-Stash, O., Martínez-Cinco, M.A., Abuharara, A., Castro, M.C., 2018. Temporal evolution of brine reinjection effects on geothermal fluids of Los Azufres, Michoacán, (Mexico) as determined by the stable isotopes of water. *Appl. Geochem.*, submitted.

Ocampo-Díaz, J., Rojas-Bribiesca, M., 2004. Production problems review of Las Tres Vírgenes geothermal field, Mexico. *Geother. Resou. Coun. Trans.* 28: 499-502.

O'Nions, R.K., Oxburgh, E.R., 1988. Helium, volatile fluxes and the development of continental crust. *Earth Planet. Sci. Lett.* 90: 331-347.

Panichi, C., Ferrara, G., Gonfiantini, R., 1977. Isotope geothermometry in the Larderello geothermal field. *Geothermics* 5: 81-88.

Paternoster, M., Oggiano, G., Sinisi, R., Caracausi, A., Mongelli, G., 2017. Geochemistry of two contrasting deep fluids in the Sardinia microplate (western Mediterranean): Relationships with tectonics and heat sources. *J. Volcanol. Geother. Res.* 336: 108-117.

Peiffer, L., Carrasco-Núñez, G., Mazot, A., Villanueva-Estrada, R.E., Inguaggiato, C., Romero, R.B., Miller, R.R., Rojas, J.H., 2018. Soil degassing at the Los Humeros geothermal field (Mexico). *J. Volcanol. Geother. Res.* 356: 163-174.

Pérez, H., J.L., M., Garduño V.H., Arce Saldaña, J.L., Garcia Tenorio, F., Castro Goeva, R., Layer, P., Saucedo Gíron, R., Martínez, C., Jimenéz Haro, A., Valdés, G., Meriggi, L., Hernández, R. 2010. Estudio vulcanológico y estructural de la secuencia estratigráfica Mil Cumbres y del campo geotérmico de Los Azufres, Mich. *Geotermia* 23: 51-63.

Pinti, D.L., Marty, B., 1998. The origin of helium in deep sedimentary aquifers and the problem of dating very old groundwaters. *Geol. Soc. London Spec. Publ.* 144: 53-68.

Pinti, D., Castro, M., Shouakar-Stash, O., Tremblay, A., Garduño, V., Hall, C., Hélie, J.-F., Ghaleb, B., 2013. Evolution of the geothermal fluids at Los Azufres, Mexico, as traced by noble gas isotopes, $\delta^{18}\text{O}$, δD , $\delta^{13}\text{C}$ and $^{87}\text{Sr}/^{86}\text{Sr}$. *J. Volcanol. Geother. Res.* 249: 1-11.

Pinti, D.L., Castro, M.C., Lopez-Hernandez, A., Han, G., Shouakar-Stash, O., Hall, C.M., Ramírez-Montes, M., 2017. Fluid circulation and reservoir conditions of the Los Humeros Geothermal Field (LHGF), Mexico, as revealed by a noble gas survey. *J. Volcanol. Geother. Res.* 333: 104-115.

Pinti, D.L., Castro, M.C., López-Hernández, A., Hernández Hernández, M.A., Richard, L., Hall, C.M., Shouakar-Stash, O., Flores-Armenta, M., Rodríguez-Rodríguez, M.A., 2018. Cerro Prieto Geothermal Field (Baja California, Mexico) – a Fossil System? Insights from a Noble Gas Study. *Applied geochemistry*, in revision.

Portugal, E., Verma, M., Barragán, R., Mañón, A., 1994. Geoquímica isotópica de ^{13}C , D, y ^{18}O de fluidos del sistema geotérmico Los Humeros Puebla (México). *Geof. Int.*, 33: 607-618.

Portugal, E., Izquierdo, G., Barragán, R., Romero, B., 2002. Hydrodynamic model of Los Humeros geothermal field, Mexico, based on geochemical, mineralogical and isotopic data. *Geof. Int.* 41: 415-420.

Pradal, E., Robin, C., 1994. Long-lived magmatic phases at Los Azufres volcanic center, Mexico. *J. Volcanol. Geother. Res.* 63: 201-215.

Prol-Ledesma, R.M., Arango-Galván, C., Torres-Vera, M.-A., 2016. Rigorous analysis of available data from Cerro Prieto and Las Tres Vírgenes geothermal fields with calculations for expanded electricity generation. *Nat. Resour. Res.* 25: 445-458.

Richet, P., Bottinga, Y., Javoy, M., 1977. A review of hydrogen, carbon, nitrogen, oxygen, sulphur, and chlorine stable isotope fractionation among gaseous molecules. *Annu. Rev. Earth Planet. Sci.* 5: 65-110.

Rouleau, E., Sano, Y., Takahata, N., Kawagucci, S., Takahashi, H., 2013. He, N and C isotopes and fluxes in Aira caldera: Comparative study of hydrothermal activity in Sakurajima volcano and Wakamiko crater, Kyushu, Japan. *J. Volcanol. Geother. Res.* 258: 163-175.

Sano, Y., Marty, B., 1995. Origin of carbon in fumarolic gas from island arcs. *Chem. Geol.* 119: 265-274.

Sano, Y., Williams S.N., 1996. Fluxes of mantle and subducted carbon along convergent plate boundaries. *Geophys. Res. Lett.* 23: 2749-2752.

Schmitt, A.K., Stockli, D.F., Niedermann, S., Lovera, O.M., Hausback, B.P., 2010. Eruption ages of Las Tres Vírgenes volcano (Baja California): A tale of two helium isotopes. *Quarter. Geochron.* 5: 503-511.

Schmitt, A.K., Martín, A., Weber, B., Stockli, D.F., Zou, H., Shen, C.-C., 2013. Oceanic magmatism in sedimentary basins of the northern Gulf of California rift. *GSA Bull.* 125, 1833-1850.

Suárez-Vidal, F., Mendoza-Borunda, R., Nafarrete-Zamarripa, L.M., Rámirez, J., Glowacka, E., 2008. Shape and dimensions of the Cerro Prieto pull-apart basin,

Mexicali, Baja California, Mexico, based on the regional seismic record and surface structures. Intern. Geol. Rev. 50: 636-649.

Tabaco, F., Verma, M., Nieva, D., Portugal, E., 1991. Características geoquímicas e isotópicas del carbono en el sistema geotérmico de Los Azufres, Mich. Geof. Int. 30: 173-182.

Tello-López, M., Torres-Rodríguez, M., 2015. Behavior of the production characteristics of the wells in the Las Tres Vírgenes, BCS, Geothermal Field, México. Proc. World Geother. Congr. 2015 Melbourne, Australia, 19-25 April 2015, p.8.

Thirlwall, M., Graham, A., Arculus, R., Harmon, R., Macpherson, C., 1996. Resolution of the effects of crustal assimilation, sediment subduction, and fluid transport in island arc magmas: Pb Sr Nd O isotope geochemistry of Grenada, Lesser Antilles. Geochim. Cosmochim. Acta 60: 4785-4810.

Torres-Rodríguez, M.A., Mendoza-Covarrubias, A., Medina-Martínez, M., 2005. An update of the Los Azufres geothermal field, after 21 years of exploitation. Proc. World Geother. Congr. 2005 Antalya, Turkey, 24-29 April 2005, p. 6.

Truesdell, A., Rye, R., Pearson Jr, F., Olson, E., Nehring, N., Whelan, J., Huebner, M., Coplen, T., 1979. Preliminary isotopic studies of fluids from the Cerro Prieto geothermal field. Geothermics 8: 223-229.

Verma, S.P., Pandarinath, K., Santoyo, E., González-Partida, E., Torres-Alvarado, I.S., Tello-Hinojosa, E., 2006. Fluid chemistry and temperatures prior to exploitation at the Las Tres Vírgenes geothermal field, Mexico. *Geothermics* 35: 156-180.

Welhan, J.A., Poreda, R., Lupton, J.E., Craig, H. (1979) Gas chemistry and helium isotopes at Cerro Prieto. *Geothermics* 8: 241-244.

Welhan, J.A., Poredai, R.J., Rison, W., Craig, H. (1988) Helium isotopes in geothermal and volcanic gases of the western United States, I. Regional variability and magmatic origin. *J. Volcanol. Geotherm. Res.* 34: 185-199.

Wen, T., Pinti, D.L., Castro, M.C., López-Hernández, A., Hall, C.M., Shouakar-Stash, O., Sandoval-Medina, F., 2018. A noble gas and $^{87}\text{Sr}/^{86}\text{Sr}$ study in fluids of the Los Azufres geothermal field, Mexico – Assessing impact of exploitation and constraining heat sources. *Chem. Geol.* 483: 426-441.

Yardley, B.W.D., Bodnar, R.J., 2014. Fluids in the Continental Crust. *Geochem. Persp.* 3, 127pp.

Zachos, J.C., Röhl, U., Schellenberg, S.A., Sluijs, A., Hodell, D.A., Kelly, D.C., Thomas, E., Nicolo, M., Raffi, I., Lourens, L.J., 2005. Rapid acidification of the ocean during the Paleocene-Eocene thermal maximum. *Science*, 308: 1611-1615.

2.10 Figures and table

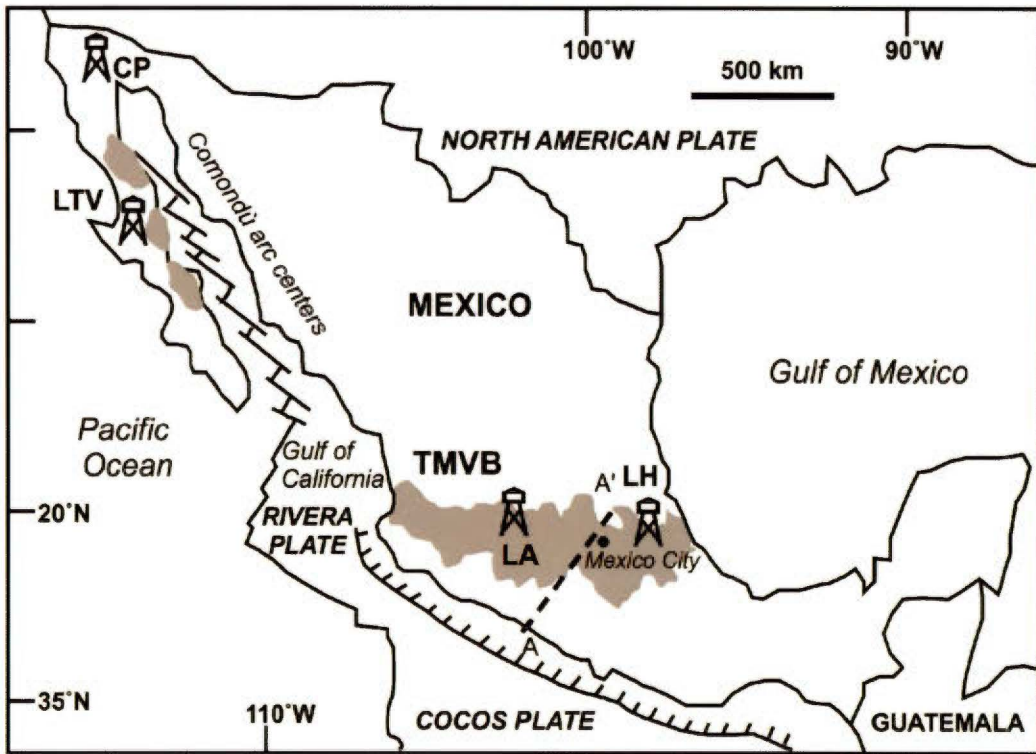


Figure 2.1. Location of the geothermal fields sampled for this study with main geodynamic features of the region. TMVB is the Trans-Mexican Volcanic Belt interpreted as the surface expression of the present-day subduction of the Cocos Plate. The Comondú arc centers are intrusions related to Miocene-time subduction which is now inactive and replaced by the Gulf of California opening. The A-A' is the transect of the lithospheric cross section of Figure 2.8.

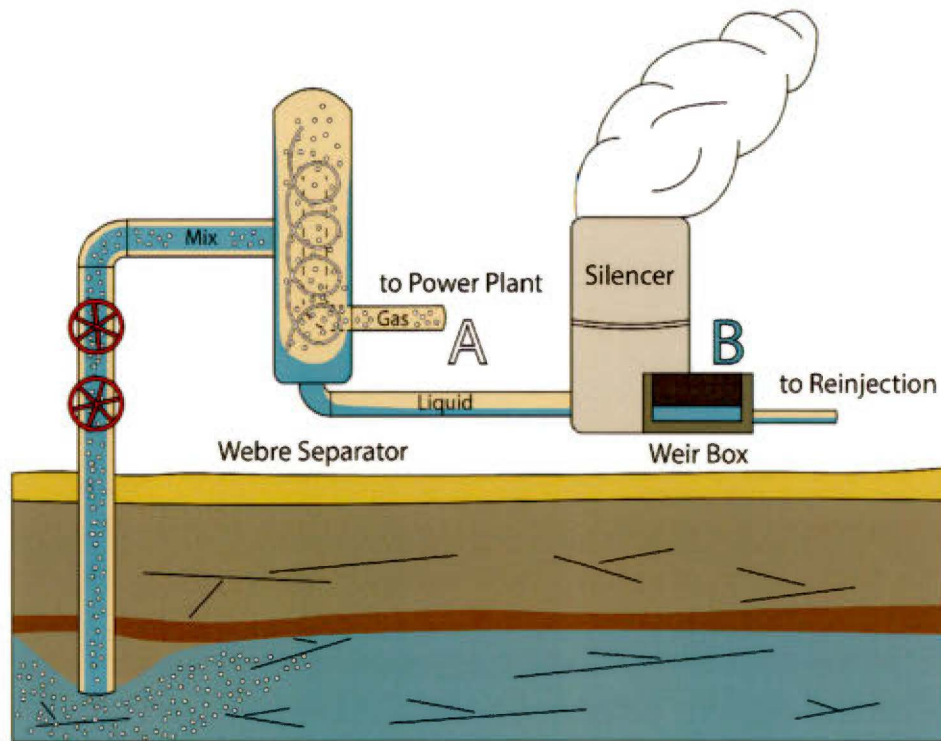


Figure 2.2. Geothermal well platform sketch showing the Webre separator, the silencer and the weirbox, with the position were gas (point A) and water (point B) samples were taken.

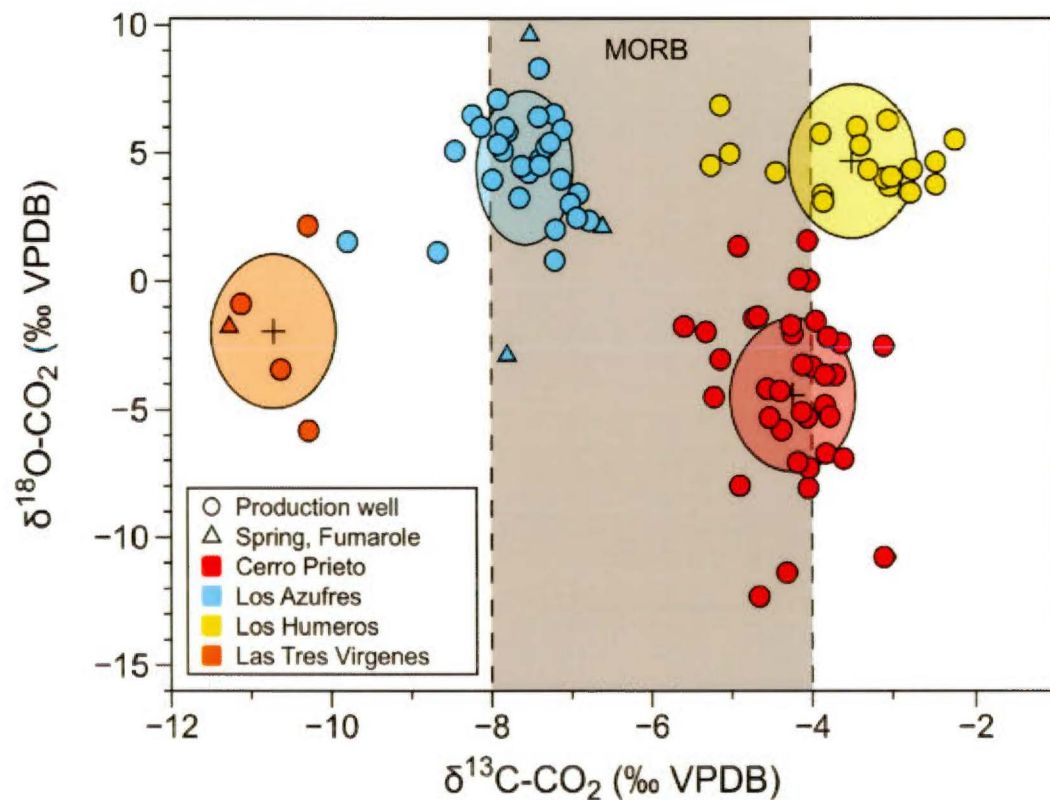


Figure 2.3. The C and O isotopic composition measured in the four geothermal fields.

Ellipsoids of different colors represents the total method variability around a mean value which is represented by the cross sign.

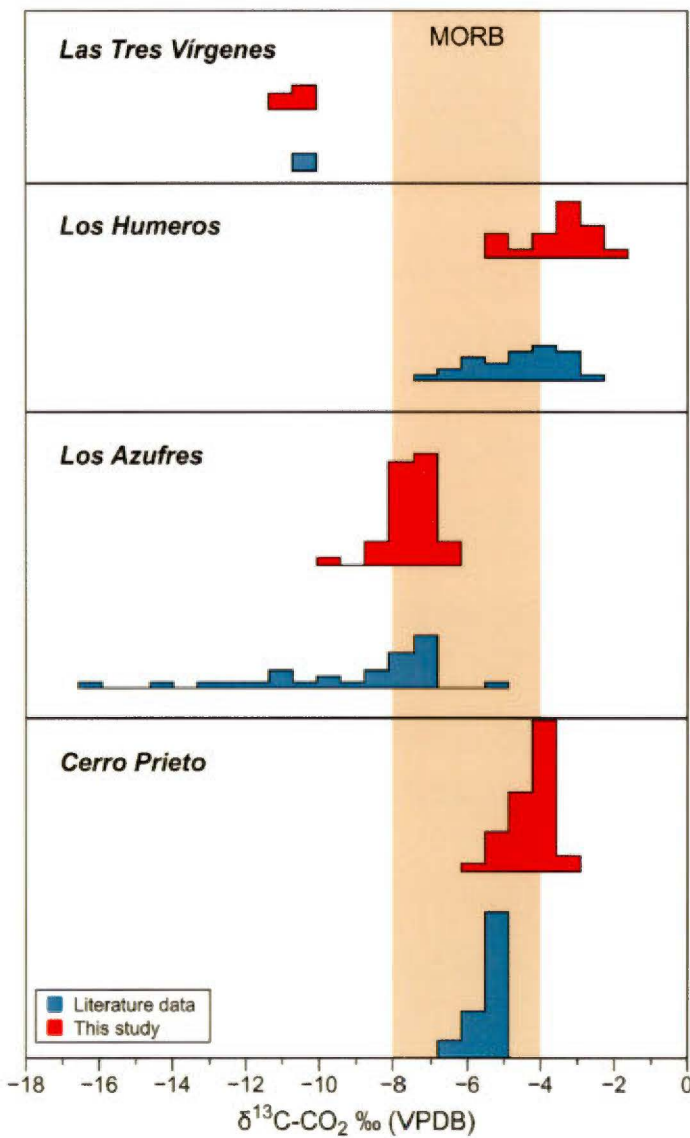


Figure 2.4. Comparison between the carbon isotopic composition, expressed as $\delta^{13}\text{C}$ (‰ vs VPDB) measured in the four geothermal fields in this study and previous literature data. To notice the extreme lighter values measured in Los Azufres by Birkle et al. (2001) which might indicate organic contamination during sampling or during analyses.

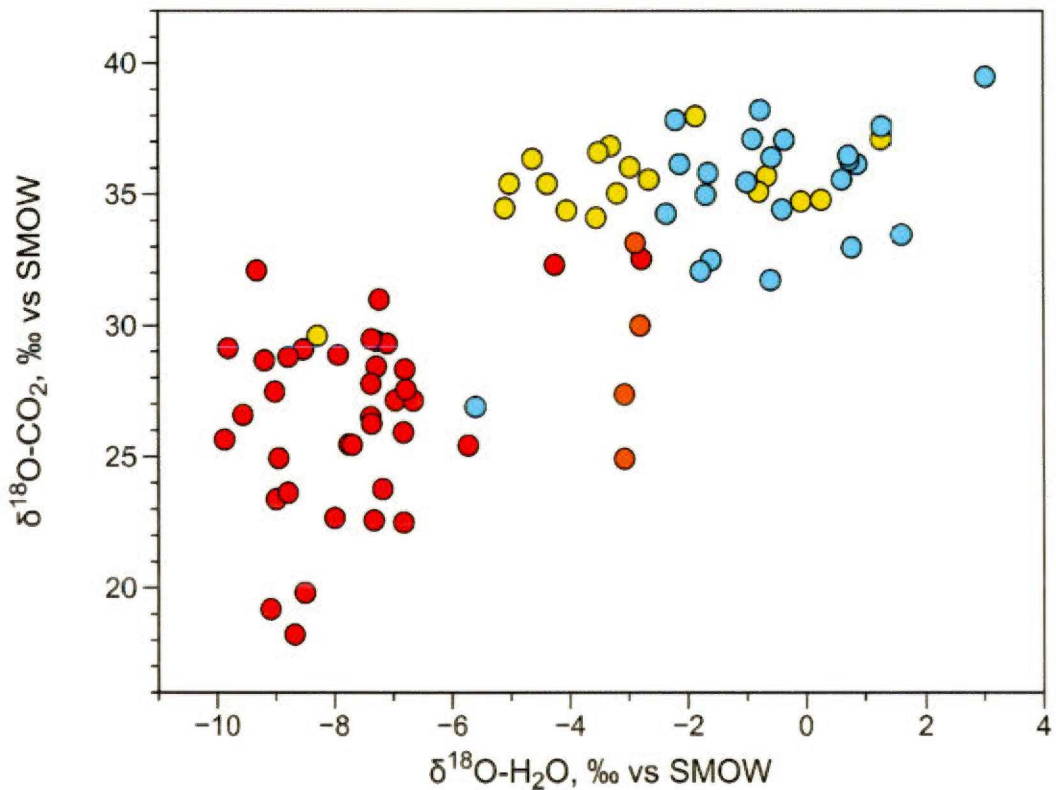


Figure 2.5. The O isotopic composition of geothermal water and CO₂ (both normalized to VSMOW) in the different geothermal field. The general trend indicates that equilibration between the two phases basically controls the oxygen isotopic signature. Scattering indicates likely the overlapping with other local processes such as exchange with silicates and carbonates in the reservoir.

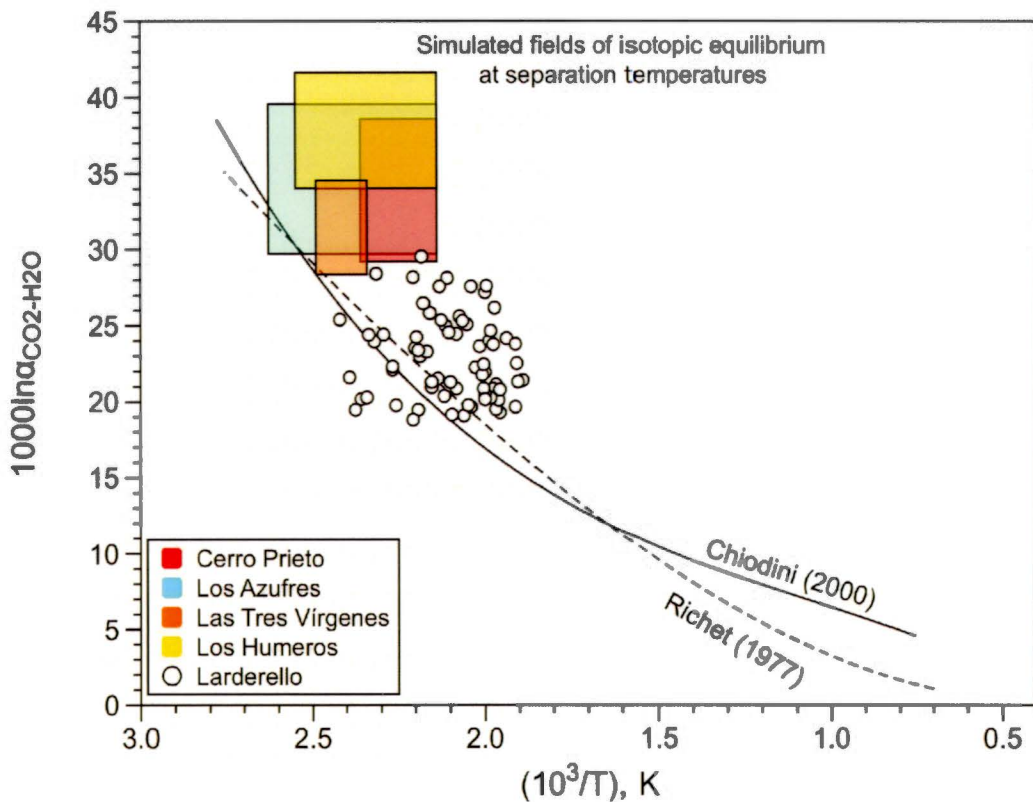


Figure 2.6. The per mil fractionation of the $\text{CO}_2\text{-H}_2\text{O}$ phase equilibration calculated at different temperatures. The curve of Chiodini et al. (2000) is calculated based on data from hot springs. The Richet et al. (1977) curve is theoretical. The boxes represent the possible range per mil fractionation between CO_2 and H_2O in the four geothermal fields studied, calculated at well separation temperatures. The data of Panichi et al. (1977) for Larderello field, Italy, is also reported for comparison.

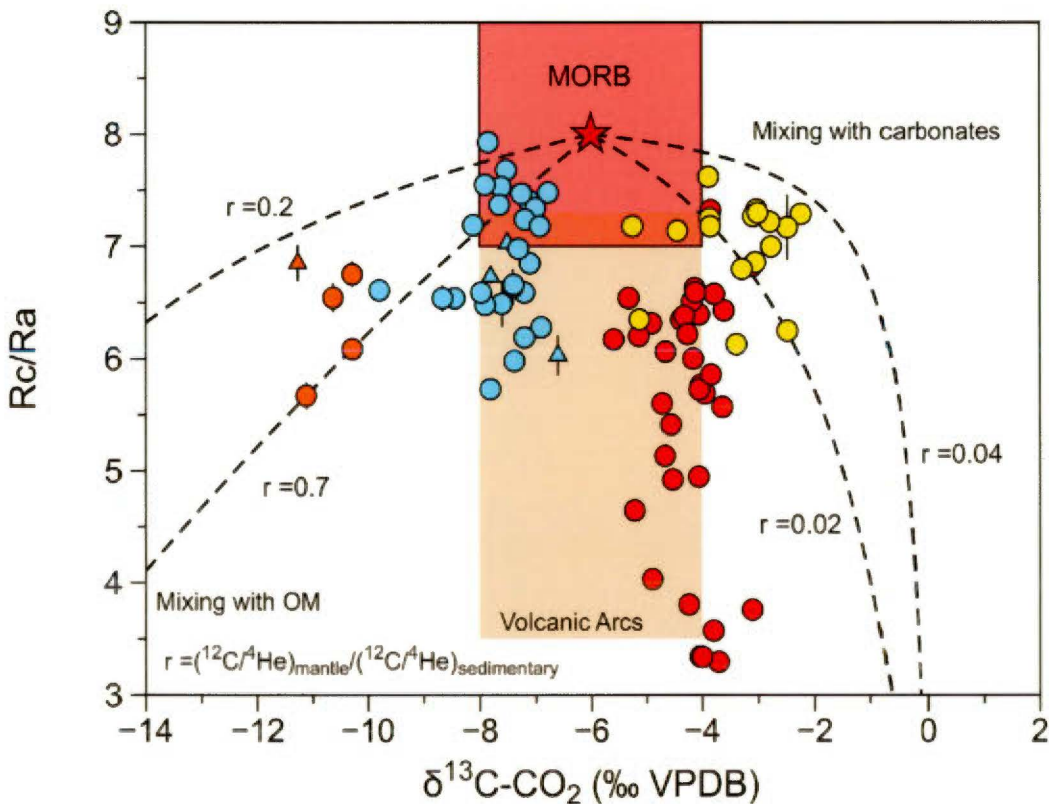


Figure 2.7. Atmosphere-corrected ${}^3\text{He}/{}^4\text{He}$ ratio measured in geothermal fluids of Mexico expressed as ratio Rc normalized to the atmospheric one Ra ($= 1.384 \times 10^{-6}$; Lupton et al., 1976) versus the $\delta^{13}\text{C}-\text{CO}_2$ measured in the same wells (see text for data sources). The dashed lines represent hyperbolas of mixing between the MORB mantle source and organic matter (OM) rich sediments and carbonates. Hyperbola curvature “ r ” is equal to the ratio $(\text{C}/\text{He})_{\text{mantle}}/(\text{C}/\text{He})_{\text{organic/carbonate}}$. Note that the Y-axis is split for sake of clarity.

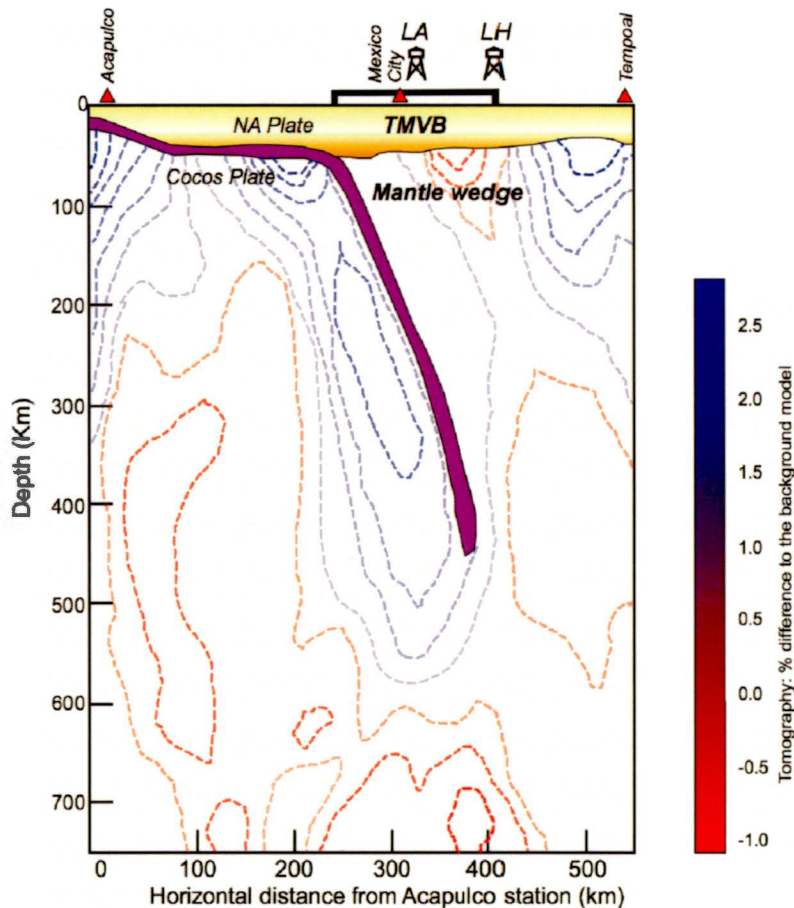


Figure 2.8. Cross section of the Coco plate subduction zone at the level of Mexico City (adapted from Pérez-Campo et al., 2008) with the relative position of the Trans Mexican Volcanic Belt (TMVB) and the geothermal fields of Los Azufres (LA) and Los Humeros (LH). Blobs of mantle material of different nature (fertilized mantle = orange and lithospheric mantle = red) are reported as possible sources of He and C in the two fields.

Tableau 2.1. The geothermal field sampled, the type of fluid collected, the year of sampling, $\delta^{13}\text{C-CO}_2$ and $\delta^{18}\text{O-CO}_2$

Geothermal field	Name (well and/or spring)	Type of sample	Sampling year	$\delta^{13}\text{C-CO}_2$ (%) VPDB)	\pm	$\delta^{18}\text{O-CO}_2$ (%) VPDB)	\pm
Cerro Prieto	CP-112	Production steam	2016	-4,72	0,01	-1,45	0,01
Cerro Prieto	CP-114	Production steam	2016	-5,59	0,00	-1,77	0,03
Cerro Prieto	CP-232	Production steam	2016	-4,03	0,00	-8,16	0,01
Cerro Prieto	CP-233	Production steam	2016	-5,32	0,01	-1,98	0,01
Cerro Prieto	CP-248	Production steam	2016	-3,83	0,01	-6,73	0,02
Cerro Prieto	CP-301	Production steam	2016	-4,91	0,01	1,35	0,02
Cerro Prieto	CP-302	Production steam	2016	-4,05	0,01	1,57	0,01
Cerro Prieto	CP-308	Production steam	2016	-4,16	0,00	0,07	0,01
Cerro Prieto	CP-311	Production steam	2016	-4,38	0,00	-5,80	0,01
Cerro Prieto	CP-318	Production steam	2016	-3,11	0,00	-2,52	0,01
Cerro Prieto	CP-345	Production steam	2016	-3,95	0,01	-1,56	0,01
Cerro Prieto	CP-346	Production steam	2016	-3,61	0,01	-6,94	0,01
Cerro Prieto	CP-404	Production steam	2016	-4,56	0,01	-4,20	0,02
Cerro Prieto	CP-419	Production steam	2016	-4,05	0,01	-8,09	0,01
Cerro Prieto	CP-423	Production steam	2016	-3,84	0,00	-4,84	0,01
Cerro Prieto	CP-501	Production steam	2016	-4,04	0,01	-7,31	0,01
Cerro Prieto	CP-505	Production steam	2016	-4,53	0,01	-5,32	0,01
Cerro Prieto	CP-508	Production steam	2016	-4,40	0,01	-4,28	0,01
Cerro Prieto	CP-509	Production steam	2016	-3,78	0,01	-5,28	0,01
Cerro Prieto	CP-512	Production steam	2016	-4,67	0,01	-1,39	0,01
Cerro Prieto	CP-513	Production steam	2016	-4,24	0,00	-2,06	0,01
Cerro Prieto	CP-542	Production steam	2016	-3,71	0,00	-3,66	0,01
Cerro Prieto	CP-207D	Production steam	2016	-3,64	0,09	-2,42	0,05
Cerro Prieto	CP-220D	Production steam	2016	-4,00	0,00	-3,34	0,02
Cerro Prieto	CP-230D	Production steam	2016	-4,18	0,01	-7,09	0,01
Cerro Prieto	CP-431D	Production steam	2016	-4,32	0,00	-11,39	0,01
Cerro Prieto	CP-522D	Production steam	2016	-4,66	0,01	-12,32	0,02
Cerro Prieto	CP-531D	Production steam	2016	-4,90	0,00	-8,00	0,01
Cerro Prieto	CP-533D	Production steam	2016	-3,80	0,00	-2,19	0,01
Cerro Prieto	CP-538D	Production steam	2016	-4,06	0,00	-5,31	0,01
Cerro Prieto	CP-545D	Production steam	2016	-5,22	0,00	-4,52	0,01
Cerro Prieto	E-24	Production steam	2016	-4,13	0,01	-5,11	0,01
Cerro Prieto	E-50	Production steam	2016	-5,14	0,01	-3,05	0,02
Cerro Prieto	E-56	Production steam	2016	-3,84	0,01	-3,67	0,00

Cerro Prieto	M-110	Production steam	2016	-4,12	0,01	-3,27	0,01
Cerro Prieto	M-126	Production steam	2016	-3,11	0,01	-10,78	0,02
Cerro Prieto	M-160	Production steam	2016	-4,26	0,00	-1,73	0,01
Los Azufres	AZ-9A	Production steam	2009	-6,90	0,12	3,40	0,01
Los Azufres	AZ-13	Production steam	2009	-7,20	0,01	6,50	0,01
Los Azufres	AZ-22	Production steam	2009	-7,20	0,03	0,80	0,01
Los Azufres	AZ-28A	Production steam	2007	-7,60	0,01	4,40	0,01
Los Azufres	AZ-33	Production steam	2007	-7,40	0,01	6,40	0,01
Los Azufres	AZ-51	Production steam	2009			6,70	0,01
Los Azufres	AZ-2A	Production steam	2014	-8,22	0,01	6,47	0,02
Los Azufres	AZ-5	Production steam	2014	-6,77	0,00	2,35	0,02
Los Azufres	AZ-6	Production steam	2014	-7,10	0,02	5,89	0,03
Los Azufres	AZ-9A	Production steam	2014	-7,84	0,06	5,07	0,01
Los Azufres	AZ-12D	Production steam	2014	-9,79	0,02	1,53	0,02
Los Azufres	AZ-13	Production steam	2014	-7,52	0,01	4,22	0,03
Los Azufres	AZ-19	Production steam	2014	-7,38	0,01	4,74	0,07
Los Azufres	AZ-25	Production steam	2014	-8,44	0,01	5,07	0,01
Los Azufres	AZ-26	Production steam	2014	-7,39	0,01	8,30	0,01
Los Azufres	AZ-28	Production steam	2014	-7,90	0,04	7,08	0,14
Los Azufres	AZ-32	Production steam	2014	-7,61	0,00	4,47	0,01
Los Azufres	AZ-33	Production steam	2014	-7,78	0,01	5,83	0,03
Los Azufres	AZ-34	Production steam	2014	-7,12	0,01	3,96	0,01
Los Azufres	AZ-38	Production steam	2014	-7,00	0,00	3,00	0,01
Los Azufres	AZ-43	Production steam	2014	-7,30	0,01	5,23	0,01
Los Azufres	AZ-46	Production steam	2014	-7,19	0,01	2,00	0,00
Los Azufres	AZ-47D	Production steam	2014	-7,25	0,00	5,39	0,01
Los Azufres	AZ-48	Production steam	2014	-8,66	0,00	1,13	0,01
Los Azufres	AZ-51	Production steam	2014	-7,64	0,03	3,24	0,06
Los Azufres	AZ-62	Production steam	2014	-8,11	0,01	6,01	0,01
Los Azufres	AZ-65	Production steam	2014	-7,81	0,01	5,98	0,03
Los Azufres	AZ-66D	Production steam	2014	-7,38	0,01	4,50	0,01
Los Azufres	AZ-67	Production steam	2014	-7,90	0,00	5,32	0,02
Los Azufres	AZ-83	Production steam	2014	-6,92	0,00	2,46	0,01
Los Azufres	AZ-89	Production steam	2014	-7,97	0,01	3,94	0,01
Los Azufres	Curutaco	Mud pod	2007	-6,60	0,00	2,10	0,01
Los Azufres	Manitaro 1	Fumarole	2009	-7,80	0,01	-2,90	0,01
Los Azufres	Maritaro 2	Fumarole	2009	-7,50	0,02	9,60	0,04
Los Humeros	H-03	Production steam	2015	-5,13	0,00	6,85	0,05
Los Humeros	H-06	Production steam	2015	-3,88	0,02	5,74	0,09
Los Humeros	H-07	Production steam	2015	-3,03	0,01	3,70	0,01
Los Humeros	H-09	Production steam	2015	-3,05	0,01	6,27	0,02
Los Humeros	H-11	Production steam	2015	-3,43	0,01	6,00	0,01
Los Humeros	H-12	Production steam	2015	-5,01	0,00	4,96	0,02
Los Humeros	H-15	Production steam	2015	-2,77	0,01	4,35	0,02

Los Humeros	H-17	Production steam	2015	-2,48	0,00	3,76	0,00
Los Humeros	H-19	Production steam	2015	-3,09	0,00	4,00	0,00
Los Humeros	H-20	Production steam	2015	-2,24	0,02	5,51	0,01
Los Humeros	H-30	Production steam	2015	-3,86	0,00	3,36	0,01
Los Humeros	H-31	Production steam	2015	-3,85	0,00	3,09	0,01
Los Humeros	H-33	Production steam	2015			5,27	0,02
Los Humeros	H-34	Production steam	2015	-5,25	0,01	4,50	0,10
Los Humeros	H-35	Production steam	2015	-4,44	0,00	4,23	0,01
Los Humeros	H-41	Production steam	2015	-3,39	0,01	5,29	0,01
Los Humeros	H-44	Production steam	2015	-2,48	0,00	4,64	0,01
Los Humeros	H-45	Production steam	2015	-2,79	0,00	3,45	0,02
Los Humeros	H-48D	Production steam	2015	-3,29	0,00	4,34	0,00
Los Humeros	H-49	Production steam	2015	-3,01	0,00	4,06	0,01
Las Tres Virgenes	El Azufre	Fumarole	2016	-11,27	0,01	-1,78	0,01
Las Tres Virgenes	LV-6	Production steam	2016	-10,28	0,01	-5,82	0,01
Las Tres Virgenes	LV-6 Inhibitor	Production steam	2016	-10,63	0,01	-3,44	0,01
Las Tres Virgenes	LV-11	Production steam	2016	-11,12	0,01	-0,89	0,01
Las Tres Virgenes	LV-13D	Production steam	2016	-10,28	0,00	2,16	0,01

CHAPITRE III

CONCLUSION GÉNÉRALE

Le but de cette maîtrise était de participer à l'amélioration des connaissances sur le carbone profond à travers l'étude du système isotopique du CO₂ ($\delta^{18}\text{O-CO}_2$, $\delta^{13}\text{C-CO}_2$) des fluides profonds de champs géothermiques mexicains. Cet outil géochimique a permis d'attribuer pour la première fois une signature isotopique bien distincte à chacun des quatre champs et de comprendre la source des fluides géothermiques.

Il a été observé que les fluides de CP-GF et LA-GF ont un $\delta^{13}\text{C-CO}_2$ correspondant à ceux alimentant les basaltes de ridges médio-océaniques (MORBs). Le CO₂ des échantillons de gaz de LH-GF et LTV-GF a respectivement une signature isotopique du carbone enrichie et appauvrie par rapport au manteau terrestre. L'étude a démontré qu'il y a eu un échange isotopique entre les fluides de LH-GF et des carbonates, alors que ceux de LTV-GF se sont mélangés avec de la matière organique. Cette dernière serait issue de la subduction de la plaque Farallon sous le continent américain. Ces deux dernières hypothèses concordent avec les valeurs de $^{87}\text{Sr}/^{86}\text{Sr}$ mesurées à chacun des sites respectifs (données non publiées).

Le $\delta^{18}\text{O-CO}_2$ dépend de la composition initiale de l'eau alimentant les fluides géothermiques, ainsi que des processus d'équilibration subséquents. Il a donc été proposé qu'une équilibration partielle entre le $^{18}\text{O-H}_2\text{O}$ et $^{18}\text{O-CO}_2$ se produit dans le séparateur. Ces résultats sont en opposition avec les observations de Chiodini (2000) qui a, quant à lui, observé une équilibration complète. Toutefois, il serait fort

improbable d'obtenir une équilibration complète dans un séparateur mécanique due au possible fractionnement cinétique causé par le taux important de fluides extraits.

Les échantillons liquides ont révélé un mélange entre des eaux météoritiques et andésitiques à CP-GF, ce qui n'était pas attendu dans un contexte de « pull-apart ». On explique cette anomalie par le fait que la réinjection de fluides équilibrés avec l'atmosphère en surface, a changé la composition isotopique magmatique initiale de l'eau vers une composition plus andésitique. L'eau andésitique est l'eau associée au volcanisme d'arc soit, de subduction. Les eaux des autres champs géothermiques semblent plutôt concordantes avec leur contexte géodynamique.

Le système de « pull-apart » présent à CP-GF semble aussi ne pas être cohérent avec les valeurs de R/Ra mesurées dans les échantillons gazeux, qui démontrent un signal purement de volcanisme d'arc. Le rapport $^3\text{He}/^4\text{He}$ (R) des fluides aurait diminué par rapport à celui de l'atmosphère (Ra) due à la production de ^4He radiogénique par désintégration d'U et de Th dans le réservoir confiné de CP-GF. Cela réduirait effectivement le ratio R/Ra et témoignerait surtout d'un réservoir qui n'a pas de recharge active et qui s'épuisera. Les fluides de LA-GF et LH-GF affichent des valeurs de R/Ra associé à un mélange mantellique pur et de volcanisme d'arc, alors que l'hélium des fluides de LTV-GF semble être originaire de volcanisme d'arc.

Bien que la variabilité du $\delta^{18}\text{O}-\text{CO}_2$ soit de $\pm 3.00 \text{ ‰}$, il a été démontré que la majeure partie de cette erreur survient à la phase d'échantillonnage. Le cumul de la variabilité des étapes subséquentes n'est seulement que de 0.5 ‰ . Les facteurs influençant la variabilité à l'échantillonnage sont : la variation de pression relativement à la ligne de production et la présence inconsistante d'eau de condensation dans les échantillons gazeux. Des solutions ont été proposées afin d'exercer un meilleur contrôle sur ces facteurs, ce qui permettrait de réduire la variabilité du $\delta^{18}\text{O}-\text{CO}_2$. Il serait ainsi un puissant outil de traçage de source des

fluides géothermiques et de leur évolution. Il est à noter que sans ce dernier outil, les fluides de LA-GF et CP-GF seraient encore indissociables (Fig. 2.3).

En conclusion, les résultats de ce mémoire de recherche ont permis de caractériser les sources des fluides des différents champs géothermiques ainsi que de comprendre leur évolution isotopique. Il a aussi permis de valoriser l'emploi du $\delta^{18}\text{O-CO}_2$ en tant que nouvel outil géochimique qui, jusqu'à aujourd'hui, était systématiquement laissé de côté. À cet outil se sont ajoutés les isotopes de l'He, qui ont permis de confirmer les résultats obtenus. Sachant que les champs géothermiques sont des analogues naturels aux sites de stockage géologiques du carbone, cette approche multi-isotopique, couplée aux mesures de concentration en CO₂ de la phase gazeuse, pourrait être utilisée afin de mieux définir les mécanismes de piégeage du CO₂ et leur pérennité.

LISTE DES RÉFÉRENCES

- Aiuppa, A., Fischer, T.P., Plank, T., Robidoux, P. et Di Napoli, R. (2017). Along-arc, inter-arc and arc-to-arc variations in volcanic gas CO₂/ST ratios reveal dual source of carbon in arc volcanism. *Earth-Science Reviews*, 168, 24-47. doi: 10.1016/j.earscirev.2017.03.005
- Aguillón-Robles, A., Calmus, T., Benoit, M., Bellon, H., Maury, R. C., Cotten, J., Bourgois, J. et Michaud, F. (2001). Late Miocene adakites and Nb-enriched basalts from Vizcaino Peninsula, Mexico: Indicators of East Pacific Rise subduction below southern Baja California?. *Geology*, 29(6), 531-534. doi: 10.1130/0091-7613(2001)029<0531:LMAANE>2.0.CO;2
- Arango-Galvan, C., Prol-Ledesma, R. M. et Torres-Vera, M. A. (2015). Geothermal prospects in the Baja California peninsula. *Geothermics*, 55, 39-57. doi: 10.1016/j.geothermics.2015.01.005
- Arellano, V. M., García, A., Barragán, R. M., Izquierdo, G., Aragón, A. et Nieva, D. (2003). An updated conceptual model of the Los Humeros geothermal reservoir (Mexico). *Journal of Volcanology and Geothermal Research*, 124(1-2), 67-88. doi: 10.1016/S0377-0273(03)00045-3
- Barragán, R. M., Arellano, V. M., Portugal, E. et Sandoval, F. (2005). Isotopic ($\delta^{18}\text{O}$, δD) patterns in Los Azufres (Mexico) geothermal fluids related to reservoir exploitation. *Geothermics*, 34(4), 527-547. doi: 10.1016/j.geothermics.2004.12.006
- Barragán Reyes, R. M., Arellano Gómez, V. M., Ramírez. Montes, M. et Tovar Aguado, R. (2010). Geoquímica isotópica ($\delta^{18}\text{O}$, δD) de fluidos de pozos del campo de Los Humeros, Pue. *Geotermia*, 23(1), 16-25. Récupéré de <https://www.researchgate.net/publication/264039427>
- Barry, P. H., Hilton, D. R., Füri, E., Halldórsson, S. A. et Grönvold, K. (2014). Carbon isotope and abundance systematics of Icelandic geothermal gases,

fluids and subglacial basalts with implications for mantle plume-related CO₂ fluxes. *Geochimica et Cosmochimica Acta*, 134, 74-99. doi: 10.1016/j.gca.2014.02.038

Bellon, H., Aguillón-Robles, A., Calmus, T., Maury, R. C., Bourgois, J. et Cotten, J. (2006). La Purísima volcanic field, Baja California Sur (Mexico): Miocene to Quaternary volcanism related to subduction and opening of an asthenospheric window. *Journal of Volcanology and Geothermal Research*, 152(3), 253-272. doi: 10.1016/j.jvolgeores.2005.10.005

Birkle, P., Merkel, B., Portugal, E. et Torres-Alvarado, I. S. (2001). The origin of reservoir fluids in the geothermal field of Los Azufres, Mexico—isotopical and hydrological indications. *Applied Geochemistry*, 16(14), 1595-1610. doi: 10.1016/S0883-2927(01)00031-2

Birkle, P., Portugal Marín, E., Pinti D. L. et Castro, M. C. (2016). Origin and evolution of geothermal fluids from Las Tres Virgenes and Cerro Prieto fields, Mexico—Co-genetic volcanic activity and paleoclimatic constraints. *Applied Geochemistry*, 65, 36-53. doi: 10.1016/j.apgeochem.2015.10.009

Bischoff, J. L., Rosenbauer, R. J. et Fournier, R. O. (1996). The generation of HCl in the system CaCl₂-H₂O: Vapor-liquid relations from 380-500 °C. *Geochimica et Cosmochimica Acta*, 60(1), 7-16. doi: 10.1016/0016-7037(95)00365-7

Bottinga, Y. (1968). Calculation of fractionation factors for carbon and oxygen isotopic exchange in the system calcite-carbon dioxide-water. *Journal of Physical Chemistry*, 72(3), 800-808. doi: 10.1021/j100849a008

Bottinga, Y. (1969). Calculated fractionation factors for carbon and hydrogen isotope exchange in the system calcite-carbon dioxide-graphite-methane-hydrogen-water vapor. *Geochimica et Cosmochimica Acta*, 33(1), 49-64. doi: 10.1016/0016-7037(69)90092-1

Bureau, H., Remusat, L., Esteve I., Pinti D.L. et Cartigny, P. (2018). The Growth of Lithospheric Diamonds. *Science Advances*, 4(6), 1-5. doi: 10.1126/sciadv.aat1602

- Calmus, T., Pallares, C., Maury, R. C., Bellon, H., Pérez-Segura, E., Aguillón-Robles, A., Carreño, A. L., Bourgois, J., Cotten, J. et Benoit, M. (2008). Petrologic diversity of Plio-Quaternary post-subduction volcanism in northwestern Mexico: An example from Isla San Esteban, Gulf of California. *Bulletin de la Société géologique de France*, 179(5), 465-481. doi: 10.2113/gssgbull.179.5.465
- Calmus, T., Pallares, C., Maury, R. C., Aguillón-Robles, A., Bellon, H., Benoit, B. et Michaud, F. (2011). Volcanic markers of the post-subduction evolution of Baja California and Sonora, Mexico: Slab tearing versus lithospheric rupture of the Gulf of California. *Pure and Applied Geophysics*, 168(8-9), 1303-1330. doi: 10.1007/s00024-010-0204-z
- Cartigny, P. (2005). Stable isotopes and the origin of diamond. *Elements*, 1(2), 79-84. doi: 10.2113/gselements.1.2.79
- Cedillo Rodríguez, F., 2000. Hydrogeologic model of the geothermal reservoirs from Los Humeros, Puebla, Mexico. *Proceedings World Geothermal Congress, Kyushu-Tohoku, Japan, May 28–June 10, 2000* (p. 6). Récupéré de <https://www.geothermal-energy.org/pdf/IGAstandard/WGC/2000/R0883.PDF>
- Chiodini, G., Allard, P., Caliro, S. et Parello, F. (2000). ^{18}O exchange between steam and carbon dioxide in volcanic and hydrothermal gases: implications for the source of water. *Geochimica et Cosmochimica Acta*, 64(14), 2479-2488. doi: 10.1016/S0016-7037(99)00445-7
- Clayton, R. N. et Steiner, A. (1975). Oxygen isotope studies of the geothermal system at Wairakei, New Zealand. *Geochimica et Cosmochimica Acta*, 39(8), 1179-1186. doi: 10.1016/0016-7037(75)90059-9
- Coplen, T. B., Brand, W., Gehre, M., Groning, M., Meijer, H., Toman, B. et Verkouteren, M. (2006). New Guidelines for $\delta^{13}\text{C}$ measurements. *Analytical Chemistry*, 78(7), 2439-2441. doi: 10.1021/ac052027c
- Coplen, T. B., 2011. Guidelines and recommended terms for expression of stable-isotope-ratio and gas-ratio measurement results. *Rapid Communications in Mass Spectrometry*, 25(17), 2538-2560. doi: 10.1002/rcm.5129

- Craig, H. et Lupton, J. E. (1976). Primordial neon, helium, and hydrogen in oceanic basalts. *Earth and Planetary Science Letters*, 31(3), 369-385. doi: 10.1016/0012-821X(76)90118-7
- Dasgupta, R. et Hirschmann, M. M. (2010). The deep carbon cycle and melting in Earth's interior. *Earth and Planetary Science Letters*, 298(1-2), 1-13. doi: 10.1016/j.epsl.2010.06.039
- De la Cruz, M.P. (1983). Estudio geológico a detalle de la zona geotérmica de Los Humeros, Pue., internal report CFE. 10-83
- Dobson, P. F. et Mahood, G. A. (1985). Volcanic stratigraphy of the Los Azufres geothermal area, Mexico. *Journal of Volcanology and Geothermal Research*, 25(3-4), 273-287. doi: 10.1016/0377-0273(85)90017-4
- Elders, W. A., Bird, D. K., Williams, A. E. et Schiffman, P. (1984). Hydrothermal flow regime and magmatic heat source of the Cerro Prieto geothermal system, Baja California, Mexico. *Geothermics*, 13(1-2), 27-47. doi: 10.1016/0375-6505(84)90005-1
- Ferrari, L., Orozco-Esquivel, T., Manea, V. et Manea, M. (2012). The dynamic history of the Trans-Mexican Volcanic Belt and the Mexico subduction zone. *Tectonophysics*, 522-523, 122-149. doi: 10.1016/j.tecto.2011.09.018
- Flores-Armenta, M. et Jaimes-Maldonado, G. (2001). The Las Tres Vírgenes Mexico geothermal reservoir. *Geothermal Resources Council Transactions*, 25, 525-534. Récupéré de <http://pubs.geothermal-library.org/lib/grc/1016972.pdf>
- Gilfillan, S. M. V., Sherwood Lollar, B., Holland, G., Blagburn, D., Stevens, S., Schoell, M., Cassidy, M., Ding, Z., Zhou, Z. et Lacrampe-Couloume, G. (2009). Solubility trapping in formation water as dominant CO₂ sink in natural gas fields. *Nature*, 458(7238), 614-618. doi: 10.1038/nature07852
- González-Partida, E., Barragán, R. M. et Nieva, D. (1993). Análisis geoquímico-isotópico de las especies carbónicas del fluido geotérmico de Los Humeros,

Puebla, México. *Geofísica Internacional*, 32(2), 299-309. Récupéré de <http://www.revistas.unam.mx/index.php/geofisica/article/view/39518/35951>

Graham, D. W. (2002). Noble gases in MORB and OIB: observational constraints for the characterization of mantle source reservoirs. *Reviews in Mineral Geochemistry*, 47, 247-318. Récupéré de https://www.researchgate.net/publication/288971654_Noble_gas_isotope_geochimistry_of_mid-ocean_ridge_and_ocean_island_basalts_Characterization_of_mantle_source_reservoirs_in_Porcelli_D_Ballentine_CJ_and_Weiler_R_eds_Reviews_in_Mineralogy_Geochemistry

Güleç, N. et Hilton, D. R., (2016). Turkish geothermal fields as natural analogues of CO₂ storage sites: gas geochemistry and implications for CO₂ trapping mechanisms. *Geothermics*, 64, 96-110. doi: 10.1016/j.geothermics.2016.04.008

Gutiérrez-Negrín, L. C. A., Izquierdo-Montalvo, G. et Aragón-Aguilar, A. (2010). Review and update of the main features of the Los Humeros geothermal field, Mexico. *Proceedings World Geothermal Congress 2010, Bali, Indonesia, April 25-29, 2010* (p. 1-7). Récupéré de <https://www.geothermal-energy.org/pdf/IGAstandard/WGC/2010/0617.pdf>

Gutiérrez-Negrín, L. C. A. (2015). Mexican geothermal plays. *Proceedings of the world geothermal congress 2015, Melbourne, Australia, April 19–25, 2015* (p. 1-9). Récupéré de <https://pangea.stanford.edu/ERE/db/WGC/papers/WGC/2015/11078.pdf>

Hayba, D. O. et Ingebritsen, S. E. (1997). Multiphase groundwater flow near cooling plutons. *Journal of Geophysical Research: Solid Earth*, 102(B6), 12235–12252. doi: 10.1029/97JB00552

Hedenquist, J. W. et Lowenstern, J. B. (1994). The role of magmas in the formation of hydrothermal ore deposits. *Nature*, 370, 519-52. doi : 10.1038/370519a0

Herrera, H. L., (2005). Actualización del modelo geológico conceptual del yacimiento geotérmico de Cerro Prieto, BC. *Geotermia*, 18(1), 37-46. Récupéré de <http://132.248.9.34/hevila/Geotermia/2005/vol18/no1/4.pdf>

- Hilton, D.R., Fischer, T.P. et Marty, B. (2002). Noble gases and volatile recycling at subduction zones. *Reviews in Mineralogy and Geochemistry*, 47, 319-370. Récupéré de <https://pubs.geoscienceworld.org/msa/rimg/article-abstract/47/1/319/235395/noble-gases-and-volatile-recycling-at-subduction?redirectedFrom=fulltext>
- Hinojosa, E. T., Verma, M. P. et González Partida, E. (2005). Geochemical characteristics of reservoir fluids in the Las Tres Virgenes, BCS, Mexico. *Proceedings world geothermal congress, Antalya, Turkey, April 24–29, 2005* (p. 1-11). Récupéré de https://www.researchgate.net/publication/267829709_Geochemical_Characteristics_of_Reservoir_Fluids_in_the_Las_Tres_Virgenes_BCS_Mexico
- Hoefs, J. (1980). *Stable isotope geochemistry* (2^e éd.), no 1980: Springer.
- Hoffman, P. F., Kaufman, A. J., Halverson, G. P. et Schrag, D. P. (1998). A Neoproterozoic snowball earth. *Science*, 281(5381), 1342-1346. doi: 10.1126/science.281.5381.1342
- Janik, C. J., Nehring, N. L., Huebner, M. A. et Truesdell, A. H. (1982). Carbon-13 variations in fluids from the Cerro Prieto geothermal system. *Conference: 4. symposium on the Cerro Prieto geothermal field, Guadalajara, Mexico, August 10-12, 1982* (p. 535-541). Récupéré de <https://www.osti.gov/servlets/purl/7369511>
- Javoy, M, Pineau, F. et Delorme, H. (1986). Carbon and nitrogen isotopes in the mantle. *Chemical Geology*, 57(1-2), 41-62. doi: 10.1016/0009-2541(86)90093-8
- Keeling, C. D. (1958). The concentration and isotopic abundances of atmospheric carbon dioxide in rural areas. *Geochimica et Cosmochimica Acta*, 13(4), 322-334. doi: 10.1016/0016-7037(58)90033-4
- Kelemen, P.B. et Manning, C.E. (2015). Reevaluating carbon fluxes in subduction zones, what goes down, mostly comes up. *Proceedings of the National*

Academy of Sciences of the United States of America, 112(E3997). doi: 10.1073/pnas.1507889112

Lan, T. F., Sano, Y., Yang, T. F., Takahata, N., Shirai K. et Pinti, D. L. (2010). Evaluating Earth degassing in subduction zones by measuring helium fluxes from the ocean floor. *Earth and Planetary Science Letters.*, 298(3–4), 317-322. doi: 10.1016/j.epsl.2010.07.049

Langmuir, C. H., Vocke Jr, R. D., Hanson, G. H. et Hart, S. R. (1978). A general mixing equation with applications to Icelandic basalts. *Earth and Planetary Science Letters*, 37(3), 380-392. doi: 10.1016/0012-821X(78)90053-5

López-Hernández, A, García Estrada, G. H., et Arellano Guadarrama, J. F. (1995). Geothermal exploration at Las Tres Vígenes, B.C.S., Mexico. *Proceedings of the 1995 World Geothermal Congress, International Geothermal Association, Florence, Italy. May 18-31, 1995* (p. 707-712). Récupéré de <https://www.geothermal-energy.org/pdf/IGAstandard/WGC/1995/2-Lopez.pdf>

Marty, B. et Jambon, A. (1987). C/He-3 in Volatile Fluxes From the Solid Earth - Implications For Carbon Geodynamics. *Earth and Planetary Science Letters*, 83(1-4), 16-26, doi: 10.1016/0012-821X(87)90047-1

Mason, E., Edmonds, M. et Turchyn, A. V. (2017). Remobilization of crustal carbon may dominate volcanic arc emissions. *Science*, 357(6348), 290-294. doi: 10.1126/science.aan5049

Moeck, I. S. et Beardmore, G. (2014). A new ‘geothermal play type’ catalog: Streamlining exploration decision making. *Proceedings of the Thirty-Ninth Workshop on Geothermal Reservoir Engineering, Stanford University, Stanford, California*. United states of America, February 24-26, 2014 (p. 1-8). Récupéré de <https://pangea.stanford.edu/ERE/pdf/IGAstandard/SGW/2014/Moeck.pdf>

Mook, W. G., Bommerson, J. C. et Staverman, W. H. (1974). Carbon isotope fractionation between dissolved bicarbonate and gaseous carbon dioxide.

Earth and Planetary Science Letters, 22(2), 169-176. doi: 10.1016/0012-821X(74)90078-8

Nehring, N. L. et D'Amore, F. (1984). Gas chemistry and thermometry of the Cerro Prieto, Mexico, geothermal field. *Geothermics*, 13(1-2), 75-89. doi: 10.1016/0375-6505(84)90008-7

Nieva, D., Fausto, J., González, J. et Garibaldi, F. (1982). Flow of Steam into the Feed- ing Zone of Wells of Cerro Prieto. *Fourth Symposium on the Cerro Prieto Field, Baja California, Mexico, August 10-12, 1982* (p. 145-152). Récupéré de https://digital.library.unt.edu/ark:/67531/metadc1101753/m2/1/high_res_d/5793903.pdf

Nieva, D., Quijano, L., Garfias, A., Barragán, R. M. et Laredo, F. (1983). Heterogeneity of the liquid phase, and vapor separation in Los Azufres (Mexico) geothermal reservoir, *Proceedings, Ninth Workshop Geothermal Reservoir Engineering, Stanford University, Stanford California, United States of America, December 13-15, 1983* (p. 253-260). Récupéré de <https://www.osti.gov/servlets/purl/889702>

Norini, G., Groppelli, G., Sulpizio, G., Carrasco-Núñez, G., Dávila-Harris, P., Pellicioli, C., Zucca, F. et De Franco, R. (2015). Structural analysis and thermal remote sensing of the Los Humeros Volcanic Complex: Implications for volcano structure and geothermal exploration. *Journal of Volcanology and Geothermal Research*, 301, 221-237. doi: 10.1016/j.jvolgeores.2015.05.014

Nuñez-Hernández, S., Pinti, D. L., López-Hernández, A., Shouakar-Stash, O., Martínez-Cinco, M. A., Abuharara, A. et Castro, M. C. (sous presse). Temporal evolution of brine reinjection effects on geothermal fluids of Los Azufres, Michoacán, (Mexico) as determined by the stable isotopes of water. *Applied Geochemistry*.

Ocampo-Díaz, J., et Rojas-Bribiesca, M. (2004). Production problems review of Las Tres Virgenes geothermal field, Mexico. *Geothermal Resources Council Transactions*, 28, 499-502. Récupéré de <http://pubs.geothermal-library.org/lib/grc/1022524.pdf>

O'Nions, R. K. et Oxburgh, E. R. (1988). Helium, volatile fluxes and the development of continental crust. *Earth and Planetary Science Letters*, 90(3), 331-347. doi: 10.1016/0012-821X(88)90134-3

Panichi, C., Ferrara, G. C. et Gonfiantini, R. (1977). Isotope geothermometry in the Larderello geothermal field. *Geothermics*, 5(1-4), 81-88. doi: 10.1016/0375-6505(77)90012-8

Paternoster, M., Oggiano, G., Sinisi, R., Caracausi, A., et Mongelli, G. (2017). Geochemistry of two contrasting deep fluids in the Sardinia microplate (western Mediterranean): Relationships with tectonics and heat sources. *Journal of Volcanology and Geothermal Research*, 336, 108-117. doi: 10.1016/j.jvolgeores.2017.02.011

Peiffer, L., Carrasco-Núñez, G., Mazot, A., Villanueva-Estrada, R. E., Inguaggiato, C., Bernard Romero, R., Rocha Miller R. et Hernández Rojas, J. (2018). Soil degassing at the Los Humeros geothermal field (Mexico). *Journal of Volcanology and Geothermal Research*, 356, 163-174. doi: 10.1016/j.jvolgeores.2018.03.001

Pérez Esquivias, H., Macías Vázquez, J. L., Garduño Monroy, V. H., Arce Saldaña, J. L., García Tenorio, F., Castro Govea, R., Layer, P., Saucedo Girón, R., Martínez, C., Jiménez Haro, A., Valdés, G. Meriggi, L. et Hernández, R. (2010). Estudio vulcanológico y estructural de la secuencia estratigráfica Mil Cumbres y del campo geotérmico de Los Azufres. *Geotermia*, 23(2), 51-63. Récupéré de <http://132.248.9.34/hevila/Geotermia/2010/vol23/no2/6.pdf>

Pinti, D. L. et Marty, B. (1998). The origin of helium in deep sedimentary aquifers and the problem of dating very old groundwaters. *Geological Society, London, Special Publications*, 144(1), 53-68. doi: 10.1144/GSL.SP.1998.144.01.05

Pinti, D. L., Castro, M. C., Shouakar-Stash, O., Tremblay, A., Garduño, V. H., Hall, C. M., Hélie, J. F. et Ghaleb, B. (2013). Evolution of the geothermal fluids at Los Azufres, Mexico, as traced by noble gas isotopes, $\delta^{18}\text{O}$, δD , $\delta^{13}\text{C}$ and

⁸⁷ Sr/86 Sr. *Journal of Volcanology and Geothermal Research*, 249, 1-11.
10.1016/j.jvolgeores.2012.09.006

Pinti, D. L., Castro, M. C., Lopez-Hernandez, A., Han, G., Shouakar-Stash, O., Hall, C. M. et Ramírez-Montes, M. (2017). Fluid circulation and reservoir conditions of the Los Humeros Geothermal Field (LHGF), Mexico, as revealed by a noble gas survey. *Journal of Volcanology and Geothermal Research*, 333-334, 104-115, doi: 10.1016/j.jvolgeores.2017.01.015

Pinti, D.L., Castro, M. C., López-Hernández, A., Hernández Hernández, M. A., Richard, L., Hall, C. M., Shouakar-Stash, O., Flores-Armenta, M. et Rodríguez-Rodríguez, M. A. (2017). Cerro Prieto Geothermal Field (Baja California, Mexico) – a Fossil System? Insights from a Noble Gas Study. *Applied Geochemistry*. en révision

Portugal, E., Verma, M. P., Barragán, R. M. et Mañón, A. (1994). Geoquímica isotópica de ¹³C, D, y ¹⁸O de fluidos del sistema geotérmico Los Humeros Puebla (México). *Geofísica internacional*, 33(4), 607-618. Récupéré de https://www.researchgate.net/profile/Rosa_Barragan/publication/259571239_Geoquimica_de_carbono_oxigeno_y_deuterio_de_fluidos_del_sistema_geotermico_de_Los_Humeros_Puebla_Mexico/links/53d2ac4f0cf228d363e94fc8/Geoquimica-de-carbono-oxigeno-y-deuterio-de-fluidos-del-sistema-geotermico-de-Los-Humeros-Puebla-Mexico.pdf

Portugal, E., Izquierdo, G., Barragán, R. M. et Romero, B. I. (2002). Hydrodynamic model of Los Humeros geothermal field, Mexico, based on geochemical, mineralogical and isotopic data. *Geofísica internacional*, 41(4), 415-420. Récupéré de <http://www.redalyc.org/articulo.oa?id=56841409>

Pradal, E. et Robin, C. (1994). Long-lived magmatic phases at Los Azufres volcanic center, Mexico. *Journal of Volcanology and Geothermal Research*, 63(3-4), 201-215. doi: 10.1016/0377-0273(94)90074-4

Prol-Ledesma, R. M., Arango-Galván, C. et Torres-Vera, M. A. (2016). Rigorous analysis of available data from cerro prieto and las tres virgenes geothermal fields with calculations for expanded electricity generation. *Natural Resources Research*, 25(4), 445-458. doi: 10.1007/s11053-016-9295-2

- Richet, P., Bottinga, Y. et Javoy, M. (1977). A review of hydrogen, carbon, nitrogen, oxygen, sulphur, and chlorine stable isotope fractionation among gaseous molecules. *Annual Review of Earth and Planetary Sciences*, 5(1), 65-110. doi: 10.1146/annurev.ea.05.050177.000433
- Rouleau, E., Sano, Y., Takahata, N., Kawagucci, S. et Takahashi, H. (2013). He, N and C isotopes and fluxes in Aira caldera: Comparative study of hydrothermal activity in Sakurajima volcano and Wakamiko crater, Kyushu, Japan. *Journal of Volcanology and Geothermal Research*, 258, 163-175. doi: 10.1016/j.jvolgeores.2013.04.003
- Sano, Y. et Marty, B. (1995). Origin of carbon in fumarolic gas from island arcs. *Chemical Geology*, 119(1-4), 265-274. doi: 10.1016/0009-2541(94)00097-R
- Sano, Y. et Williams, S. N. (1996). Fluxes of mantle and subducted carbon along convergent plate boundaries. *Geophysical Research Letters*, 23(20), 2749-2752. doi: 10.1029/96GL02260
- Schmitt, A. K., Stockli, D. F., Niedermann, S., Lovera, O. M. et Hausback, B. P. (2010). Eruption ages of Las Tres Vírgenes volcano (Baja California): a tale of two helium isotopes. *Quaternary Geochronology*, 5(5), 503-511. doi: 10.1016/j.quageo.2010.02.004
- Suárez-Vidal, F., Mendoza-Borunda, R., Nafarrete-Zamarripa, L. M., Rámirez, J. et Glowacka, E. (2008). Shape and dimensions of the Cerro Prieto pull-apart basin, Mexicali, Baja California, México, based on the regional seismic record and surface structures. *International Geology Review*, 50(7), 636-649. doi: 10.2747/0020-6814.50.7.636
- Tabaco, F., Verma, M. P., Nieva, D. et Portugal, E. (1991). Características geoquímicas e isotópicas del carbono en el sistema geotérmico de Los Azufres, Mich. *Geofísica Internacional*, 30(3), 173-182. Récupéré de <http://www.revistas.unam.mx/index.php/geofisica/article/view/39456>

Tello-López, M. R. et Torres-Rodríguez, M. A. (2015). Behavior of the Production Characteristics of the Wells in the Las Tres Vírgenes, B. C. S., Geothermal Field, México. *Proceedings World Geothermal Congress, Melbourne, Australia, April 19-25, 2015* (p. 1-8). Récupéré de <https://pangea.stanford.edu/ERE/db/WGC/papers/WGC/2015/24018.pdf>

Thirlwall, M. F., Graham, A. M., Arculus, R. J., Harmon, R. S. et Macpherson, C. G. (1996). Resolution of the effects of crustal assimilation, sediment subduction, and fluid transport in island arc magmas: Pb Sr Nd O isotope geochemistry of Grenada, Lesser Antilles. *Geochimica et Cosmochimica Acta*, 60(23), 4785-4810. doi: 10.1016/S0016-7037(96)00272-4

Torres-Rodríguez, M. A., Mendoza-Covarrubias, A. et Medina-Martínez, M. (2005). An update of the Los Azufres geothermal field, after 21 years of exploitation. *Proceedings World Geothermal Congress, Antalya, Turkey, April 24-29, 2005* (p. 1-8). Récupéré de <https://www.geothermal-energy.org/pdf/IGAstandard/WGC/2005/0916.pdf>

Truesdell, A. H., Rye, R. O., Pearson Jr, F. J., Olson, E. R., Nehring, N. L., Whelan, J. F., Huebner, M. A. et Coplen, T. B. (1979). Preliminary isotopic studies of fluids from the Cerro Prieto geothermal field. *Geothermics*, 8(3-4), 223-229. doi: 10.1016/0375-6505(79)90044-0

Verma, S. P., Pandarinath, K., Santoyo, E., González-Partida, E., Torres-Alvarado, I. S. et Tello-Hinojosa, E. (2006). Fluid chemistry and temperatures prior to exploitation at the Las Tres Vírgenes geothermal field, Mexico. *Geothermics*, 35(2), 156-180. doi: 10.1016/j.geothermics.2006.02.002

Welhan, J. A., Poreda, R., Lupton, J. E. et Craig, H. (1979). Gas chemistry and helium isotopes at Cerro Prieto. *Geothermics*, 8(3-4), 241-244. doi: 10.1016/0375-6505(79)90046-4

Welhan, J. A., Poredai, R. J., Rison, W. et Craig, H. (1988). Helium isotopes in geothermal and volcanic gases of the western United States, I. Regional variability and magmatic origin. *J. Volcanol. Geotherm. Res.* 34(3-4), 185-199. doi: 10.1016/0377-0273(88)90032-7

Wen, T., Daniele L. P., Castro, M. C., López-Hernández, A., Hall, C. M., Orfan Shouakar-Stash, O. et Sandoval-Medina, F. (2018). A noble gas and $^{87}\text{Sr}/^{86}\text{Sr}$ study in fluids of the Los Azufres geothermal field, Mexico—Assessing impact of exploitation and constraining heat sources. *Chemical Geology*, 483, 426-441. doi: 10.1016/j.chemgeo.2018.03.010

Yardley, B. W. D. et Bodnar, R. J., 2014. Fluids in the Continental Crust. *Geochemical Perspectives*, 3(1), 1-127. doi 10.7185/geochempersp.3.1

Zachos, J. C., Röhl, U., Schellenberg, S. A., Sluijs, A., Hodell, D. A., Kelly, D. C., Thomas, E., Nicolo, M., Raffi, I. et Lourens, L. J. (2005). Rapid acidification of the ocean during the Paleocene-Eocene thermal maximum. *Science*, 308(5728), 1611-1615. doi: 10.1126/science.1109004